GUIDEBOOK

Sedimentation on the Serravalian forebulge shelf of the Polish Carpathian Foredeep

Guide to field trip A1 • 21–22 June 2015

Stanisław Leszczyński, Wojciech Nemec

31st IAS
Meeting of Sedimentology
Kraków, Poland • June 2015

ORLEN Upstream

www.orlenupstream.pl

DRILLING

RESERVOIR ENGINEERING

E&P PROJECT ANALYSIS

PRODUCTION PROCESSES

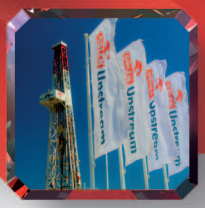

GEOLOGY

GEOPHYSICS

ENVIRONMENTAL PROTECTION HSE

ORLEN GROUP. FUELLING THE FUTURE.

ORLEN Upstream Sp. z o.o.
ul. Prosta 70 | 00-838 Warszawa
Tel.: +48 22 778 02 00 | Fax: +48 22 395 49 69

Sedimentation on the Serravalian forebulge shelf of the Polish Carpathian Foredeep

Stanisław Leszczyński[1], Wojciech Nemec[2]

[1]Jagiellonian University, Poland (stan.leszczynski@uj.edu.pl)
[2]University of Bergen, Norway (wojtek.nemec@uib.no)

Route (Fig. 1): From Kraków we drive NE by road 79 (direction Sandomierz) to Ostrowce (ca. 82 km from Kraków) and then northwards by local roads to Stopnica and by road 756 to Szydłów (**stops A1.1** and **A1.2**). From Szydłów we turn W by road 765 to Chmielnik (19 km), then turn S by road 73; after 4 km at Śladków Mały (near roadside inn 'Wilczyniec') we turn left to local dirt road leading (ca. 1 km) to the agrotourism farm Rafał Gawlik (**stop A1.3**, **lunch & accommodation**). After lunch, we drive back to Chmielnik and by road 78 and local roads reach **stop A1.4** between Sędziejowice and Chomentówek. We return to Chmielnik and Śladków Mały (road 73) and by local eastward road reach **stop A1.5** near Suskrajowice. From there we return to the agrotourism farm in Śladków Mały for the night. On the second day, we use local roads and road 73 to reach **stops A1.6–A1.13** (distance ca.12 km) between Chmielnik and Busko Zdrój. We drive further by road 73 to Busko Zdrój and continue to Kraków by road 776 (105 km).

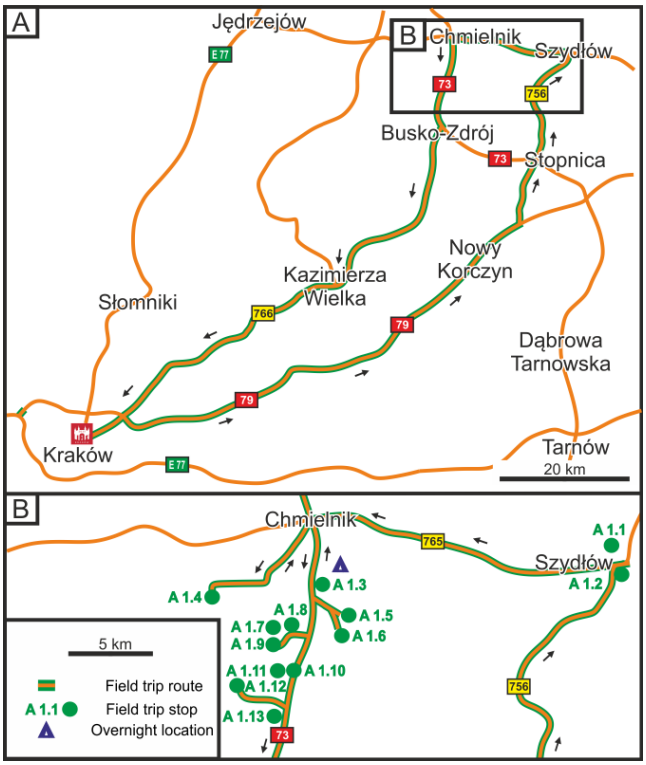

Fig. 1. Route map of field trip A1.

Introduction to the trip

Forebulge shelf depozone and peripheral unconformity

Peripheral bulge, or forebulge, is the outer marginal part of a foredeep basin formed by lithospheric flexure (Beaumont, 1981; Flemings & Jordan, 1989). Its width and bathymetric gradient depend upon the flexural rigidity of the underlying lithosphere and the orogen structural growth. The forebulge basinward flank is a flexural depozone that straddles the transition between the outer craton area of denudation and the deep-water realm of foredeep syncline. This shelf depozone receives sediment

Leszczyński, S. & Nemec, W., 2015. Sedimentation on the Serravalian forebulge shelf of the Polish Carpathian Foredeep. In: Haczewski, G. (ed.), *Guidebook for field trips accompanying IAS 31st Meeting of Sedimentology held in Kraków on 22nd–25th of June 2015*. Polish Geological Society, Kraków, pp. 5–23.
Guidebook is available online at www.ing.uj.edu.pl/ims2015

eroded off the adjacent craton, while its accommodation space is controlled by both tectonics and eustatic sea-level changes (Catuneanu *et al.,* 1998; Catuneanu and Sweet, 1999).

Forebulge depozones and foredeep peripheral unconformities have been little studied, as they are poorly exposed or virtually non-preserved. The simplified numerical models of a steady-state forebulge retreat, though most instructive, have inadvertently suggested that the resulting peripheral unconformity is a simple time-transgressive onlap feature (e.g., see Flemings and Jordan, 1989, figs 6–8, 11; Sinclair *et al.,* 1991, figs 8–13; Sinclair, 1997, fig. 2; Allen and Allen, 2005, fig. 4.33). This idealized model is by no means a universal stratigraphic guide, not least because the episodes of forebulge retreat alternate with episodes of its arching (Flemings and Jordan, 1990; Jordan and Flemings, 1991; Ettensohn, 1994; DeCelles and Currie, 1996; Currie, 1997). The sediment supply and eustatic sea-level changes come further into play, and their immediate impact is much stronger on the forebulge shelf than in the foredeep interior. The forebulge shelf is subject to frequent bathymetric changes and its shoreline is prone to rapid shifting, which renders the peripheral unconformity and onlap pattern far more intricate than portrayed by idealized 'steady-state' model.

These aspects of composite peripheral unconformity have been recently addressed by a sedimentological study of the Miocene forebulge shelf of the Polish Carpathian Foredeep (Leszczyński and Nemec, 2015). The topic of excursion A1 is to demonstrate some of the results of this study, which compares local sequence stratigraphy with the eustatic record and focuses on the deposits of a prominent mid-Serravalian clastic wedge known as the Chmielnik Formation. The forebulge shelf has a well-defined palaeogeographic gradient and its deposits have a negligible tectonic tilt, while showing several rapid shoreline shifts. High-resolution stratigraphy of regional palaeogeographic development remained difficult to reconstruct because of widely isolated outcrops. Biostratigraphic data are of little help, as the whole clastic wedge is within a single nannoplankton biozone. The excursion aims are: (1) to review the range of sedimentary systems in a classic forebulge depozone, as recognized from a typical mosaic of isolated outcrops; (2) to demonstrate how the local palaeoenvironmental changes can be regionally correlated on the logical basis of sequence stratigraphy; and (3) to show how this sedimentological approach can reveal the stratigraphic anatomy of a composite peripheral unconformity in a foredeep basin and shed light on the orogen-driven forebulge kinematics and basin tectonic history.

Geological setting of the excursion area

The excursion area is located in the outer central segment of the Polish Carpathian Foredeep (Fig. 2A), at the land-locked northwestern extremity of Miocene epicontinental Paratethys Sea (Fig. 2B). The flexural foredeep evolved by a northward thrusting of the Carpathian orogen against the margin of the European Platform,

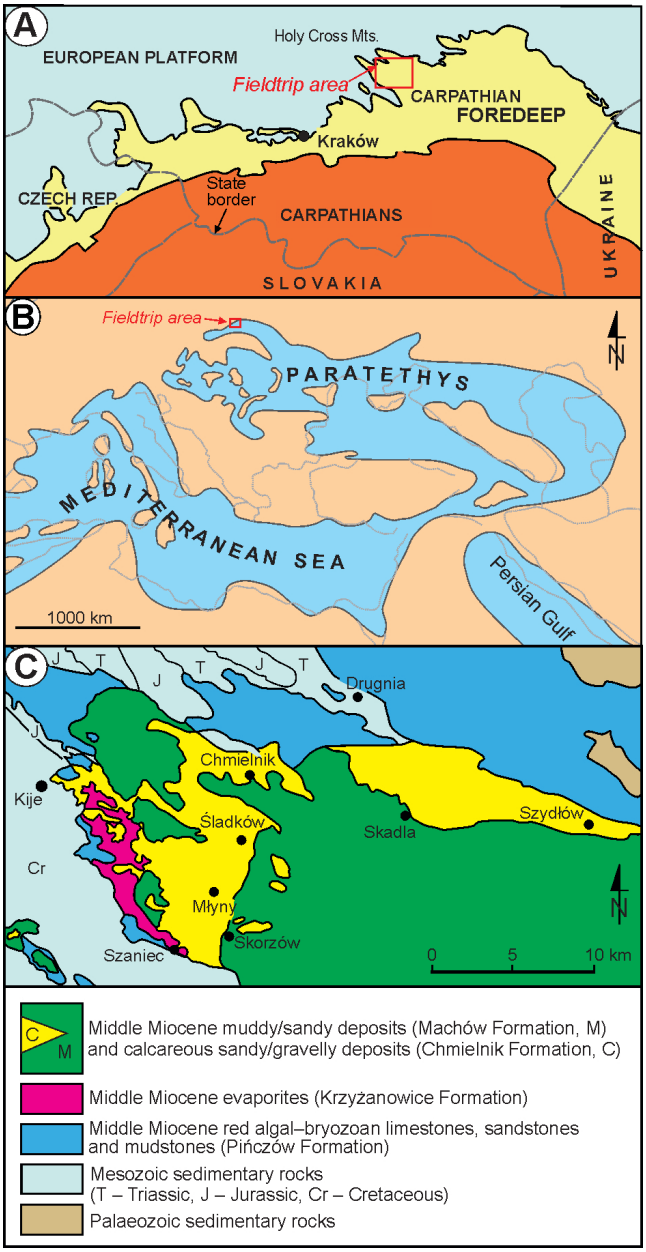

Fig. 2. (**A**) Location of the field trip area in the Polish Carpathian Foredeep. (**B**) The field trip area in a broader palaeogeographic framework of the Miocene Paratethys (map modified from Reuter *et al.*, 2012). (**C**) Geological map of the field-trip area without Quaternary cover (modified from Instytut Geologiczny, 1961).

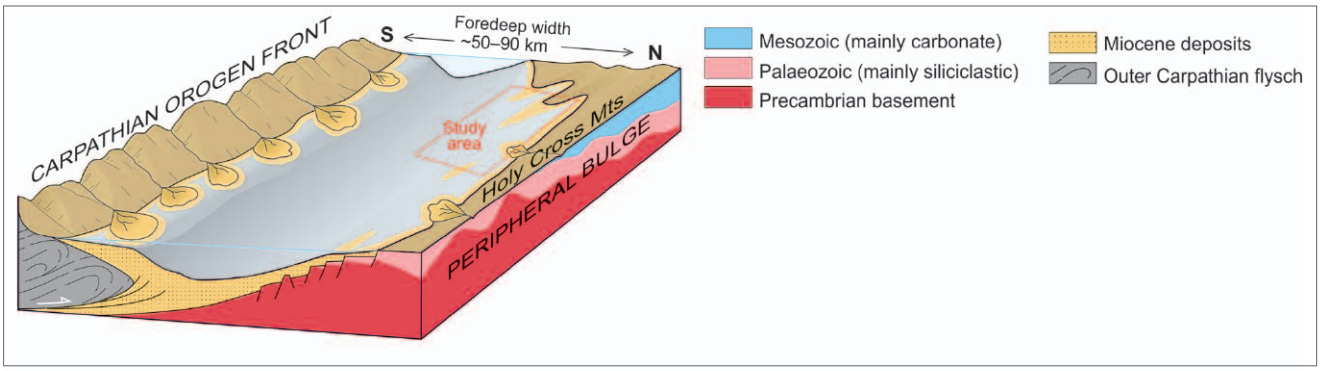

Fig. 3. Schematic model of the central segment of the Miocene Polish Carpathian Foredeep with an approximate location of the field trip area (studied by Leszczyński and Nemec, 2015). Note the peripheral bulge flank and its general N–S bathymetric gradient, with a roughly linear northern shoreline and a digitated western shoreline related to bedrock topographic ridges.

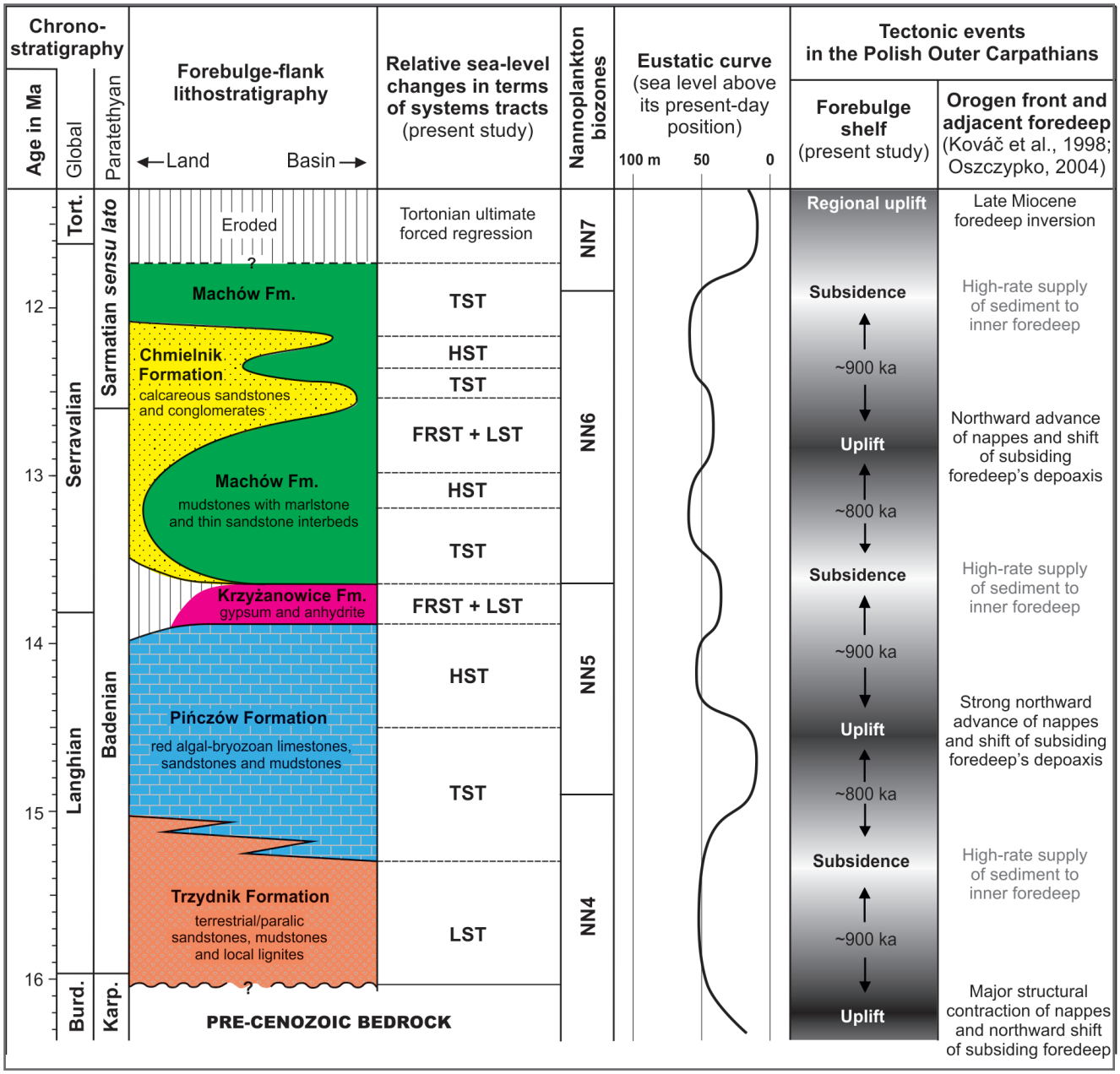

Fig. 4. Middle Miocene lithostratigraphy of the northern margin of Polish Carpathian Foredeep (based on Dudziak and Łaptaś, 1991; Jasionowski *et al.*, 2004; Stachacz, 2007; De Leeuw *et al.*, 2010) with a corresponding interpretation of relative sea-level changes in terms of systems tracts, the Tethyan calcareous nannoplankton zones (after Hilgen *et al.*, 2012) and eustatic sea-level curve (after Snedden & Liu, 2010; adjusted to the Neogene time scale of Hilgen *et al.*, 2012). The letter symbols of systems tracts (terminology after Helland-Hansen, 2009): FRST — forced-regressive systems tract; HST — normal-regressive highstand systems tract; LST — normal-regressive lowstand systems tract; TST — transgressive systems tract. The timing of orogen main thrusting events is after Kováč *et al.* (1998) and Oszczypko (2004).

where a peripheral bulge formed (Fig. 3). The forebulge crest is the bedrock ridge of the Holy Cross Mountains to the north of the excursion area. The forebulge shelf depozone has a pre-defined palaeogeographic gradient with land area to the north and deep-water realm to the south (Fig. 3). The foredeep in its inner part accumulated a thick (1–3 km) succession of early to middle Miocene deep-marine to deltaic siliciclastic deposits, which were partly overridden by the Carpathian thrust wedge (Fig. 3; Porębski et al., 2003; Oszczypko et al., 2006). In the outer part of the foredeep, a northwards-thinning succession of middle Miocene biogenic limestones, evaporites and clastic deposits (Fig. 4, left), up to a few hundred metres thick, onlapped the denudated Palaeozoic–Mesozoic bedrock of the peripheral bulge (Figs 2C, 3; Alexandrowicz et al., 1982).

The Chmielnik Formation

The Chmielnik Formation (Alexandrowicz *et al.,* 1982), originally referred to as the 'detrital Sarmatian' (Kowalewski, 1958; Rutkowski, 1976), consists of shallow-marine coarse clastic deposits that form the uppermost part of sedimentary succession in this central segment of the forebulge flank (Fig. 4). The formation occurs at the surface (Fig. 2C), beneath a thin cover of Quaternary deposits, and its isolated outcrops are mainly abandoned quarry pits. Sedimentation was controlled by both the orogen tectonism (Rutkowski, 1976, 1981; Czapowski and Studencka, 1990; Wysocka, 1999) and the Paratethys responses to eustatic sea-level changes (Rögl, 1998, 1999; Piller *et al.,* 2007). Marine sedimentation in this part of the foredeep commenced in the early Langhian (Alexandrowicz *et al.,* 1982; Jasionowski, 1997) with paralic deposits of the Trzydnik Formation and carbonates of the Pińczów Formation (Fig. 4). The evaporative drawdown recorded by the Krzyżanowice Formation (Fig. 4; Kwiatkowski, 1972; Peryt, 2006) was followed by another marine transgression, represented by the muddy Machów Formation (Fig. 4; Oszczypko *et al.,* 1992; Oszczypko, 1998). The Chmielnik Formation (Fig. 4) is a coarse-clastic nearshore equivalent of the Machów Formation that first extended basinwards and then was rapidly covered by the latter in the middle Serravalian (Jasionowski, 2006). The Tortonian witnessed a gradual withdrawal of the sea towards the southeast (Dziadzio, 2000; Dziadzio *et al.,* 2006).

The Chmielnik Formation forms a stratigraphic coarse-clastic wedge within the muddy Machów formation and pinches out basinwards. In cratonward direction, it covers unconformably the Pińczów Formation (Dudziak and Łaptaś, 1991; Garecka and Olszewska, 2011) or locally also the pre-Miocene bedrock (Rutkowski, 1976) (Fig. 2C). The Chmielnik Formation has been studied since the 19th century (see review by Czapowski, 1984) and dated to the Paratethyan latest Badenian–early Sarmatian (Fig. 4) on the basis of foraminifers (Łuczkowska, 1964; Olszewska, 1999), macrofauna (Czapowski and Studencka, 1990) and calcareous nannonplankton (Peryt, 1987; Dudziak and Łaptaś, 1991; Garecka and Olszewska, 2011). The main part of the formation, up to 30 m thick (Czapowski, 2004), has an estimated time-span of ca. 1.1 Ma in the upper part of biozone NN6 (Fig. 4; Dudziak and Łaptaś, 1991; Peryt, 1997). The formation basal part (Fig. 4), with an estimated mean thickness of less than 10 m and a time-span of ca. 450 ka, has been recognized only locally (Dudziak and Łaptaś, 1991) and dated to the transition of biozones NN5–NN6 and lower NN6.

The deposits of the Chmielnik Formation range on a local scale from weakly cemented, nearly pure siliciclastic sandstones to well-cemented calcarenites and calcirudites with or without significant siliciclastic admixture, including interbeds of calcareous to non-calcareous mudstones and sporadic pelitic, microbial serpulid or coralline-algal limestones (Rutkowski, 1976; Czapowski, 1984; Czapowski and Studencka, 1990). Sarmatian marine fauna is locally mixed with transported plant leaves and terrestrial/freshwater gastropods (Zastawniak, 1974, 1980; Górka, 2008; Stworzewicz *et al.,* 2013). The deposits have generally been considered to be of nearshore origin, passing basinwards into offshore mudstones, with palaeocurrent directions in the azimuth range of 100–190° (Rutkowski, 1976; Czapowski, 1984; Czapowski and Studencka, 1990; Łaptaś, 1992), indicating a combination of seaward and alongshore sediment transport. However, sedimentological documentation was sparse and the exact pattern of relative sea-level changes, shoreline shifts and palaeogeographic development remained controversial and unclear.

According to the study by Leszczyński and Nemec (2015), the Chmielnik Formation consists of fluvio-deltaic, foreshore and shoreface deposits with a range of

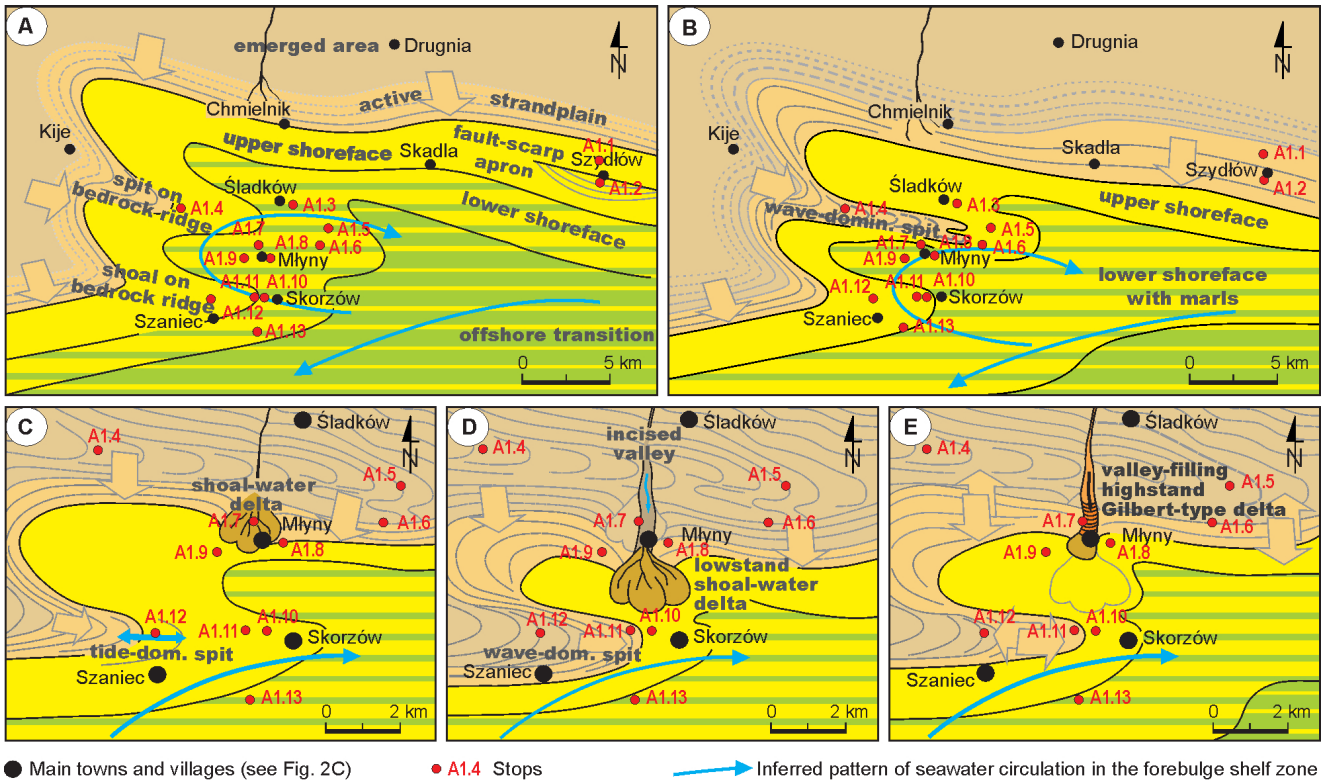

Fig. 5. Palaeogeographic reconstruction of the development of Chmielnik Fm. in the fieldtrip area (see regional setting in Fig. 2). Slightly modified from Leszczyński and Nemec (2015). (**A**) The mid-Serravalian regression begins with an encroachment of lower- to upper-shoreface sands onto the muddy offshore-transition deposits of the Machów Fm. (see Fig. 4). The northern shoreline passed Chmielnik and approaches locality A1.1, while the digitated western shoreline remains outside the study area. Western littoral sand shoals form on ESE-trending bedrock ridges, and fault scarp-attached sand bars form at localities A1.1 and A1.2. (**B**) The regressive northern shoreline approaches locality A1.3, while a wave-dominated spit bar extends to the ESE through localities A1.4–6 to become merged with the regressive shoreline. (**C**) A zoomed-in sketch showing the northern shoreline reaching localities A1.7–9, where beach deposits and sandy shoal-water delta form, while a tide-dominated new sandy spit begins to extend eastwards through locality A1.12. (**D**) The northern shoreline reaches locality A1.8 when forced regression forms an incised fluvial valley at locality A1.7 with a corresponding gravelly shoal-water lowstand delta developing to the south (Fig. 20) and a lowstand beach forming at locality A1.9. The east-advancing spit bar concurrently extends from locality A1.12 to localities A1.11 and A1.13, while becoming wave-dominated. (**E**) Minor marine transgression occurs, followed by a highstand normal regression, whereby the incised valley at locality A1.7 is drowned and filled by Gilbert-type bayhead delta, while the adjacent strandplain at locality A1.8 is concurrently inundated and covered with regressive upper-shoreface deposits. The subsequent major transgression forms a transgressive shoreface unit at all localities and brings back muddy offshore-transition deposits of Machów Fm. to the study area (see profile in Fig. 4, top).

large littoral sand bars, all enveloped in muddy offshore-transition deposits. The formation comprises a poorly exposed basal transgressive wedge and two subsequent regressive wedges (Fig. 4, left), which jointly reveal an active interplay of orogen-driven forebulge tectonism, sediment supply and 3rd-order eustatic cycles (Fig. 4, right). Facies analysis indicates rapid shoreline shifts and allows palaeogeographic reconstruction of environmental changes (Fig. 5). A similar interplay of the main controlling factors is recognizable in the whole mid-Miocene sedimentary succession that accumulated in the forebulge depozone, with the tectonic cycles of alternating forebulge uplift and subsidence spanning ca. 800–900 ka and the episodes of uplift correlating with the main pulses of Carpathian orogen thrusting (Fig. 4, right). The study by Leszczyński and Nemec (2015) has demonstrated that the forebulge depozone is an extreme case of an accommodation-controlled shelf, where the combination of tectonism, eustasy and sediment supply has a profound palaeogeographic, environmental and stratigraphic impact. Detailed facies analysis of forebulge deposits may allow recognition of the relative role of these factors.

The Miocene composite peripheral unconformity in the Polish Carpathian Foredeep (Fig. 6B) differs markedly from the idealized model of a 'steady-state' flexural onlap (Fig. 6A), as do also most other documented worldwide cases. It is therefore suggested that the forebulge sedimentary successions and peripheral unconformities, instead of being simplified in terms of the idealized model, should

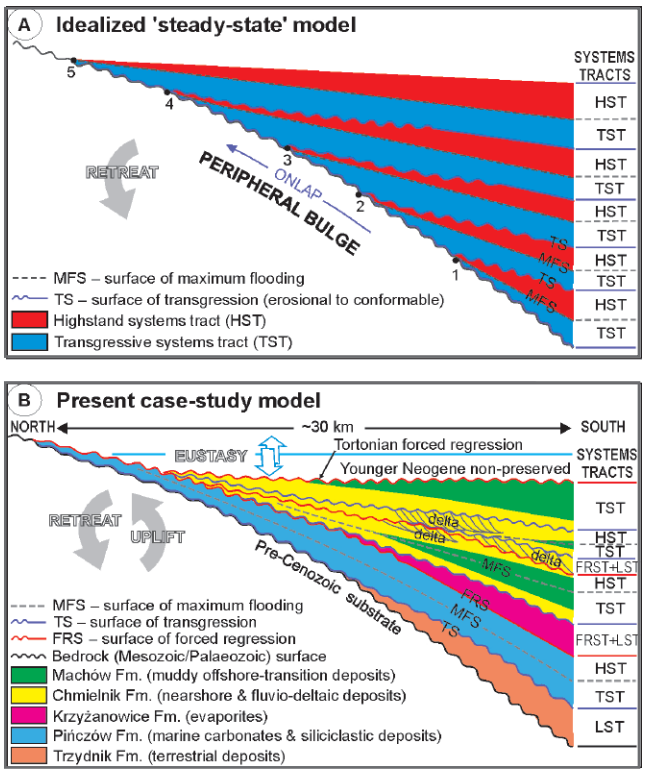

Fig. 6. Dynamic stratigraphy of foredeep peripheral unconformity. (**A**) An idealized 'steady-state' onlap portrayed by forebulge continuous-retreat models. (**B**) The present case model for the Miocene peripheral unconformity in the central segment of the Polish Carpathian Foredeep (see stratigraphy in Fig. 4). From Leszczyński and Nemec (2015).

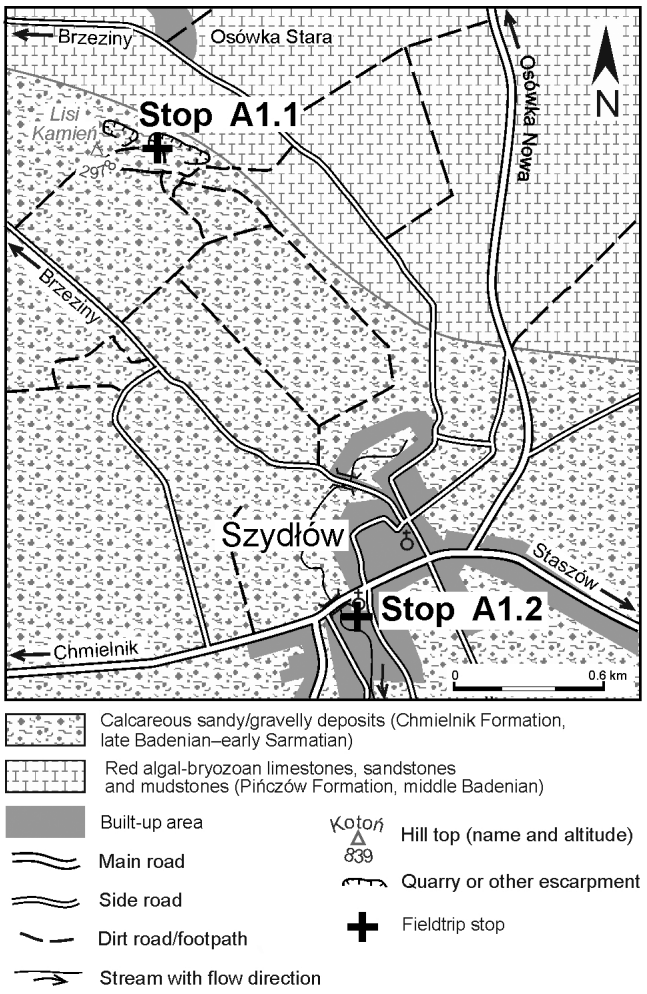

Fig. 7. Geological map showing detailed location of the fieldtrip stops A1.1 and A1.2.

rather be studied in detail as they bear a high-resolution record of regional events and give unique insights into the local role of tectonism, eustasy and sediment yield. Analysis of the stratigraphic anatomy of peripheral unconformity aids reconstruction of the forebulge kinematics and foredeep tectonic history (see Leszczyński and Nemec, 2015).

Stop descriptions

All outcrops in this field excursion are easily accessible from the car parking places, within a walking distance of 5–15 minutes. The excursion focuses on the isolated outcrops of the Chmielnik Formation in the Szydłów–Sędziejowice–Zwierzyniec area (Fig. 1B), and its aim is to demonstrate and discuss the spectrum of sedimentary systems on a classical forebulge shelf. It will be discussed further how the events recorded in the local outcrop sections can be correlated according to the basic principles of sequence stratigraphy to reveal the shelf depositional history (see also Leszczyński and Nemec, 2015). [The ensuing text refers also to Plates 1–3 given as attachments in the electronic version of the guide.]

Stop A1.1 Abandoned sandstone quarry on the Lisi Kamień hill near the village of Osówka Stara

(50°36′20″N, 20°59′29″ E; Fig. 7); access by local dirt road.

The deposits (coarse-grained to pebbly calcarenites) are upper-shoreface to foreshore facies representing the late Serravalian shoreline of the Chmielnik Fm. at its early-regressive northern location (north of locality A1.2). The shoreface deposits form giant foreset on the inferred hanging wall of an east-striking syndepositional normal growth-fault and appear to have been deformed by rotational sliding while burying the active fault escarpment (Fig. 8). They are covered with south-prograding gravelly foreshore deposits, which also seem to have been affected by a subsequent minor reactivation of the fault. The synsedimentary extensional faulting, better documented by Łaptaś (1992) in coeval deposits farther to the east, indicates forebulge doming (see e.g., Agarwal *et al.*, 2002).

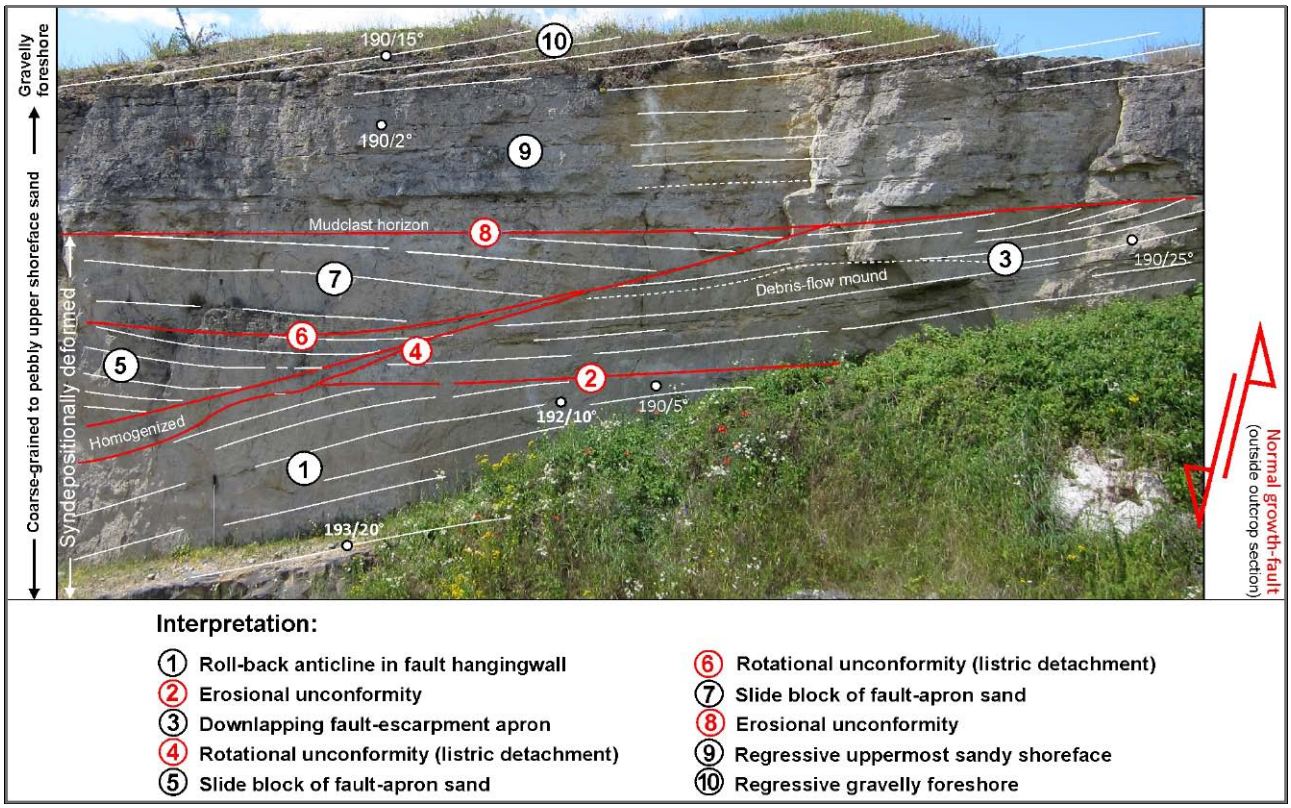

Fig. 8. Interpreted portion of the NW wall of outcrop at stop A1.1 (Figs 1B, 7). The main part of succession (units 1–7) consists of upper-shoreface deposits accumulated as a giant foreset on the hanging wall of an inferred normal fault, with evidence of syndepositional rotational sliding. The covering top part (units 9 and 10) comprises south-prograding uppermost shoreface and relic gravelly foreshore deposits. The walking stick (lower left) is 1 m.

Stop A1.2 Escarpment of the Ciekąca brooklet in Szydłów

(50°35′18″ N, 21°00′05″ E; Fig. 7) at the western foot of the church-hosting local hill.

Another fault scarp-attached, large littoral calcarenitic bar with giant-scale, south-dipping foreset stratification and listric rotational slide detachments (Fig. 9). This east-striking sandstone body is isolated and lenticular in plan-view shape, estimated to be a few kilometres long and less than 1 km wide (Łaptaś, 1992). Its foreset is at least 13 m thick (top unpreserved). The strata inclination of 25–35° decreases tangentially to 15–20° at the transition to a subhorizontal (<10°) bottomset of finer-grained sandstones (base unexposed). The bar foreset shows numerous reactivation surfaces and common

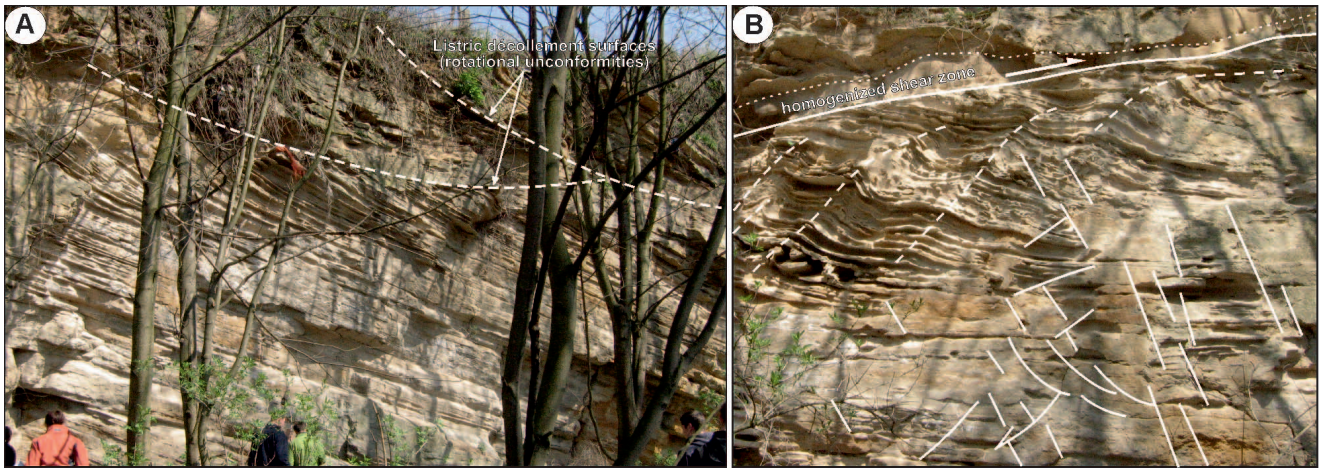

Fig. 9. (**A**) Giant foreset stratification with listric rotational slides in a fault scarp-attached littoral sand bar at stop A1.2 (Figs 1B, 7). (**B**) Close-up detail of the same bar, showing a listric detachment smeared with homogenized sand, shear-induced drag folds (dashed lines) and synsedimentary fractures; the outcrop portion is ~5 m high. (See also similar coeval cases in Plate 1.). From Leszczyński and Nemec (2015).

synsedimentary deformation in the form of slump folds, listric detachments (Fig. 9A), related drag folds and soft-sediment fracturing (Fig. 9B). The bottomset, recognized in wells, is underlain by a heterolithic succession of fine-grained sandstones intercalated with mudstone and marlstone layers (Łaptaś, 1992), considered to be lower-shoreface deposits. Similar other coeval large bars attached to syndepositional fault escarpments were recognized by Łaptaś (1992) over a distance of 30 km to the east (see Plate 1).

Stop A1.3 Rock escarpments around the Gawlik family agrotourism farm in Śladków Mały

(50°34′53″ N, 20°05′14″ E; Fig. 10)

The sandstones and conglomerates here represent the regressive upper shoreface and foreshore of the Chmielnik Fm. at the palaeoshoreline younger location to the south of stops A1.1 and A1.2. The well-sorted deposits have a variable proportion of calciclastic and siliciclastic components, reflected in their varied degree of cementation. The horizontally bedded arenites in the outcrop lower part (Fig. 11A) show mainly planar parallel stratification with numerous subhorizontal truncations, but also wave-ripple cross-lamina-

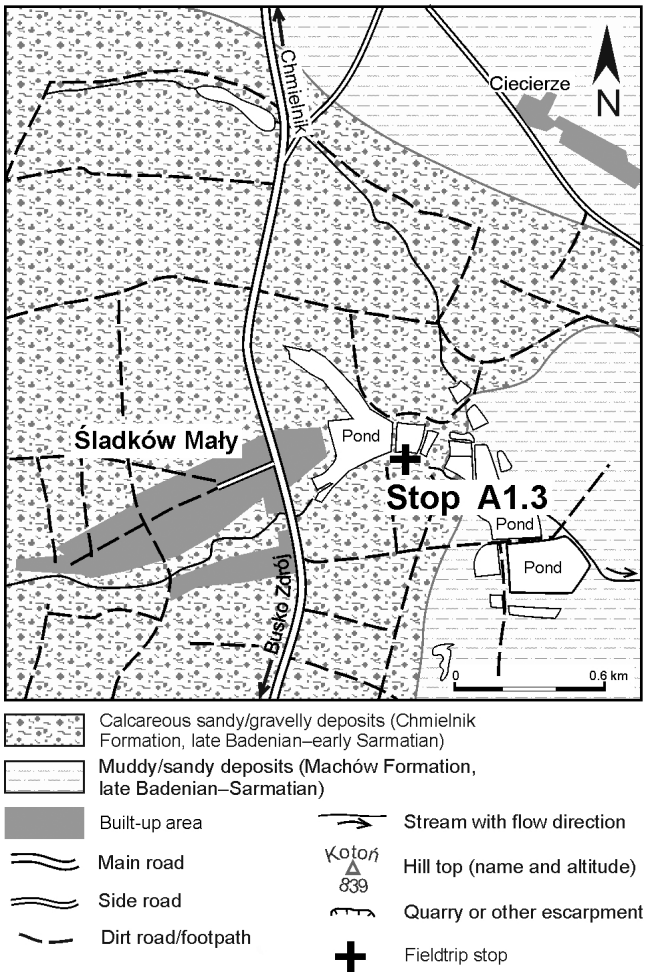

Fig. 10. Geological map showing detailed location of field-trip stop A1.3 (modified from Instytut Geologiczny, 1961).

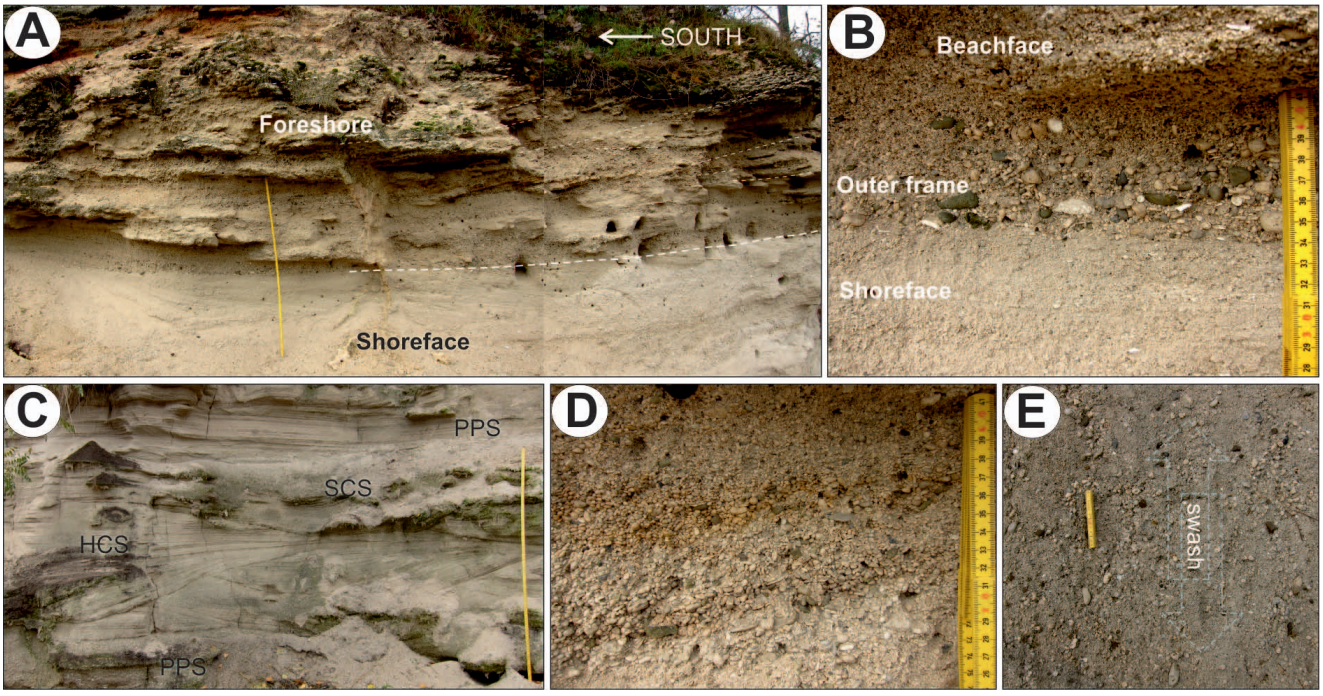

Fig. 11. (**A**) Interpreted portion of the outcrop at stop A1.3 (Figs 1B, 10); the measuring stick (scale) is 1 m. (**B**) Close-up view of the sharp contact between foreshore and underlying shoreface deposits; the visible part of measuring stick is 14 cm. (**C**) Close-up view of shoreface sandstones showing planar parallel (PPS), swaley (SCS) and hummocky stratification (HCS); the measuring stick is 1 m. (**D**) Close-up detail of inclined foreshore strata composed of well-sorted very coarse-grained sand rich in granules and small pebbles; the visible part of measuring stick is 16 cm. (**E**) Bedding surface of foreshore deposits with swash-aligned pebbles and diffuse sand ribbons; the measuring stick is 13 cm.

tion and both swaley and hummocky stratification in the lowest part (Fig. 11C). The range of stratification types and the lack of argillaceous interlayers indicate deposition in a perennially wave-worked upper shoreface environment (Clifton, 1981; Hampson, 2000). Planar parallel stratification alternating with subordinate wave-ripple cross-lamination indicates fair-weather wave action with generally high but fluctuating orbital velocities (Clifton et al., 1971; Komar and Miller, 1975). The associated trough cross-stratification represents linguoid or lunate dunes driven by wave-generated littoral currents (Clifton and Dingler, 1984). Swaley and hummocky stratifications indicate deposition by storm-generated combined flows (Dumas and Arnott, 2006).

The sandstones show slight upward coarsening and are overlain by a solitary foreset of granule to fine-pebble conglomerate, 120–140 cm thick, with strata inclined southwards at 15–25° (Fig. 11A). The basal part of tangential foreset shows coarse-grained sand rich in outsized subspherical pebbles and small cobbles (Fig. 11B). Sediment is polymictic, generally well rounded and well sorted (Fig. 11D), with the stratification surfaces showing dip-aligned pebbles and diffuse sand ribbons (Fig. 11E). These deposits are thought to represent a mixed sand-gravel foreshore system dominated by moderate- to high-energy waves (Massari and Parea, 1988). The sandy toeset rich in outsized gravel is the beach 'outer-frame' facies of Bluck (1999). The diffuse dip-parallel lineation on foreset surfaces is a signature of beach swash (Allen, 1982). These gravelly deposits are interpreted as a regressive strandplain that prograded rapidly to the south.

Stop A1.4 Rock escarpments on the eastern side of the asphalt road between Sędziejowice and Chomentówek

(50°34′23″ N, 20°39′42″ E; Fig. 12)

The outcrops show foreset and bottomset deposits of an early-stage coarse-grained spit platform built towards the ESE in a relatively deep (≥10 m) shoreface water. The northern outcrop (Fig. 12) exposes the upper part of a thick foreset (>6 m; topset non-preserved) of steeply east-inclined cross-strata of well-sorted, granule-rich very coarse-grained sand. The lower part of the foreset and its transition to a less inclined bottomset are exposed

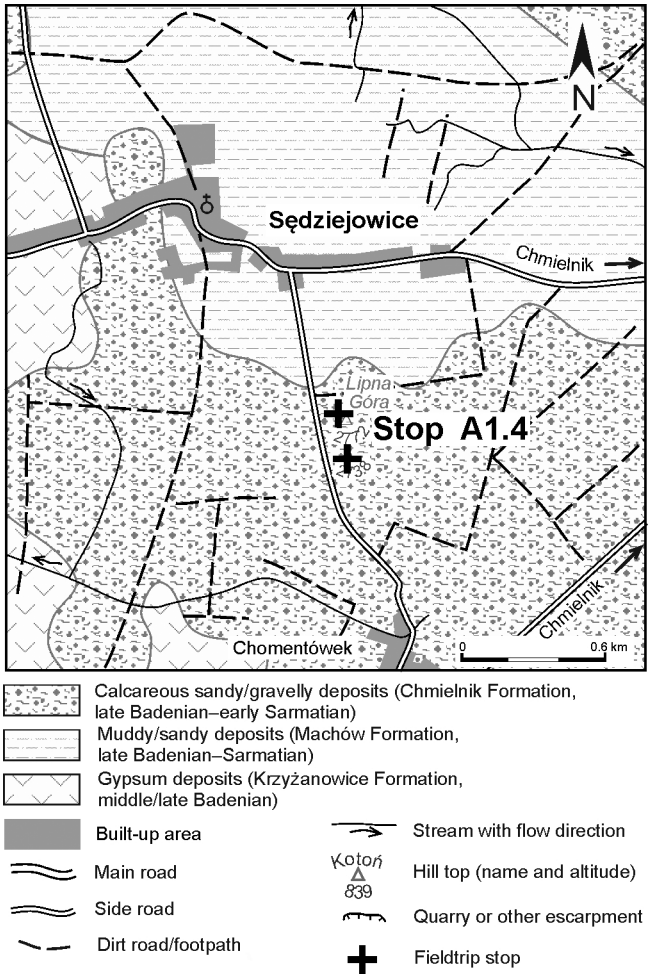

Fig. 12. Geological map showing detailed location of field-trip stop A1.4 (modified from Instytut Geologiczny, 1961).

in the southern outcrop (Fig. 12). The foreset abounds in internal truncation and reactivation surfaces (Fig. 13A). The bottomset consists of fine- to medium-grained sandstones with planar parallel stratification and both swaley and hummocky strata sets (Fig. 13B).

The deposits are thought to represent the subaqueous platform (*sensu* Meistrell, 1972) of a coarse-grained spit system similar to those described by Nielsen *et al.* (1988) and Nielsen and Johannessen (2008) (see Plate 2A). The wave-dominated spit prograded towards the ESE and is estimated to have been about 1.5 km wide and 11 km long, reaching the eastern stops A1.5 and A1.6 (Figs 1B, 12). The foreset truncation and reactivation surfaces are due to both storm erosion and gravitational collapses. The bottomset consists of upper-shoreface deposits, yet abnormally inclined (10–15°), as is generally characteristic of advancing spit systems (Nielsen and Johannessen, 2008).

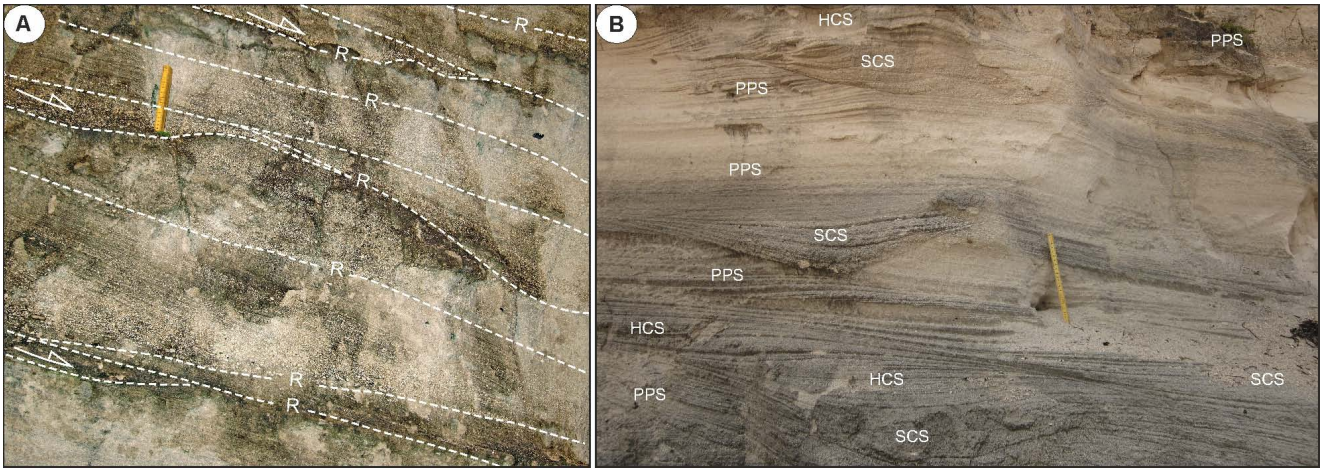

Fig. 13. (**A**) Foreset of granule sandstone with numerous reactivation surfaces (R) in a spit-bar platform at stop A1.4 (Figs 1B, 12; see Plate 2A); arrows indicate coarse-grained massive sediment avalanches; the measuring stick is 13 cm. (**B**) The upper-shoreface sandstones of spit platform bottomset at the same locality, with planar parallel (PPS), swaley (SCS) and hummocky (HCS) stratification; the direction of spit progradation is away from the viewer; the measuring stick is 21 cm.

Stop A1.5 Sand pit near Suskrajowice

(50°34′23″ N, 20°39′42″ E; Fig. 14)

The outcrop shows the most distal part of the same wave-dominated spit system (stop A1.4) that extended itself towards the ESE along the south-advancing and shoaling general shoreface (see Fig. 5B). The spit platform here, built in shallower water, is strikingly different. The inclined (15–18°) beds of upper-shoreface sandstones show planar parallel stratification and obliquely accreted dune cross-strata sets (Fig. 15) – similar as observed in the platforms of other shoal-water spits (Nielsen and Johannessen, 2008; see Plate 2B).

Stop A1.6 Sand pit in Borzykowa

(50°34′23″ N, 20°39′42″ E; Fig. 14).

The outcrop shows sandy deposits of the southern flank of the same distal shoal-water spit system (stop A1.5) with east-inclined (15–18°), parallel-stratified shoreface facies overlain by foreshore facies (Fig. 16A). The lower part of spit platform contains thin interbeds of calcareous mud (Fig. 16B), indicating deposition in a lower shoreface environment. The sparsely preserved coarse-sandy foreshore deposits at the top represent the spit-bar ridge.

Stop A1.7 Escarpment along a fish pond near the local shop in Młyny

(50°33′08″ N, 20°43′30″ E; Fig. 17).

The north–south outcrop section, 150 m long (Fig. 18), shows basal marl-interlayered mid-shoreface sandstones (poorly exposed) overlain by a sandy shoal-water delta and incised further by a fluvial valley that was flooded by

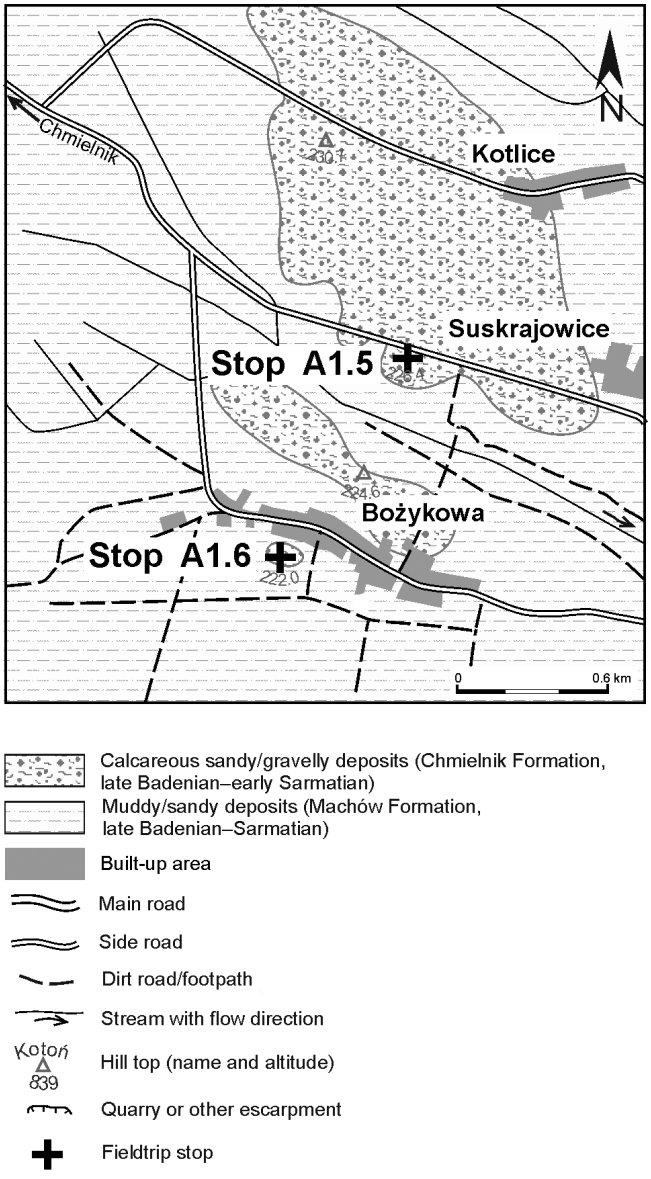

Fig. 14. Geological map showing detailed location of the field-trip stops A1.5 and A1.6 (modified from Instytut Geologiczny, 1961).

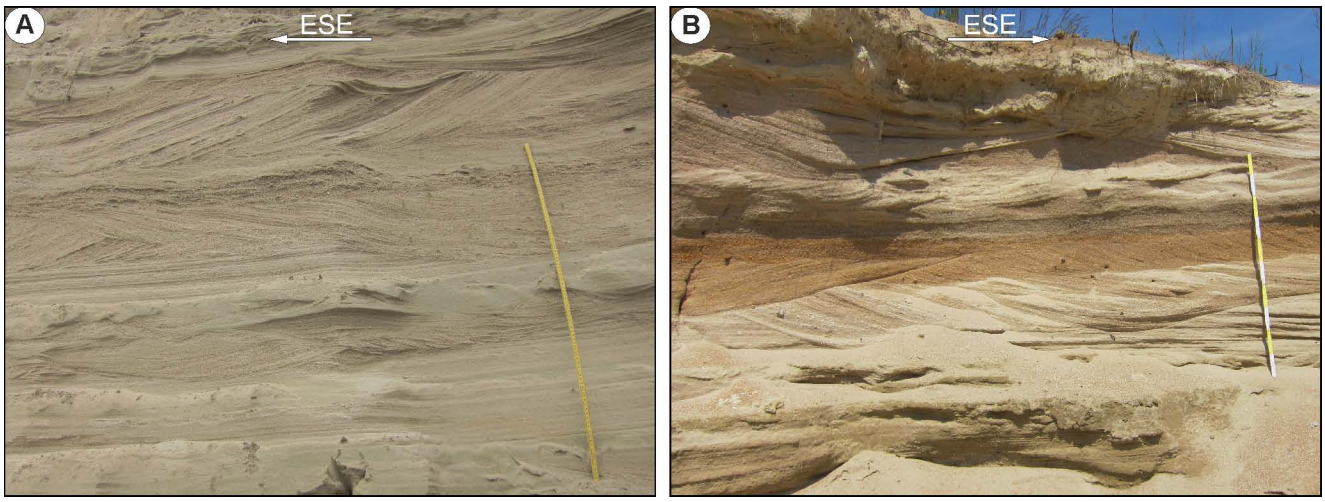

Fig. 15. (**A**, **B**) Close-up views of two opposite outcrop walls showing upper shoreface sandstones of spit-bar platform at stop A1.5 (Figs 1B, 14); note in **A** the alternation of trough cross-stratification and inclined (10–20°) planar parallel stratification. The spit bar prograded to the ESE and the dune cross-strata sets were accreted obliquely (see Plate 2B). The measuring stick is 1 m.

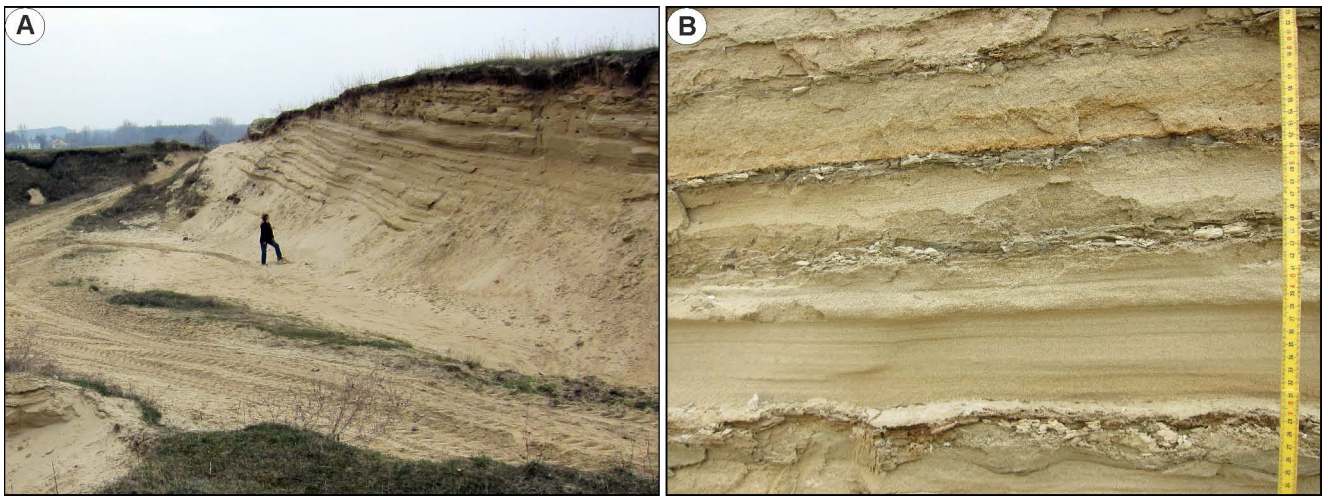

Fig. 16. Sandy deposits of spit-bar platform at stop A1.6 (Figs 1B, 14). (**A**) Lower- to upper-shoreface deposits, remarkably inclined towards the ENE, overlain by relic foreshore deposits in the sand-pit western wall. (**B**) Close-up detail of lower-shoreface deposits with mudstone interlayers. The visible part of measuring stick is 40 cm.

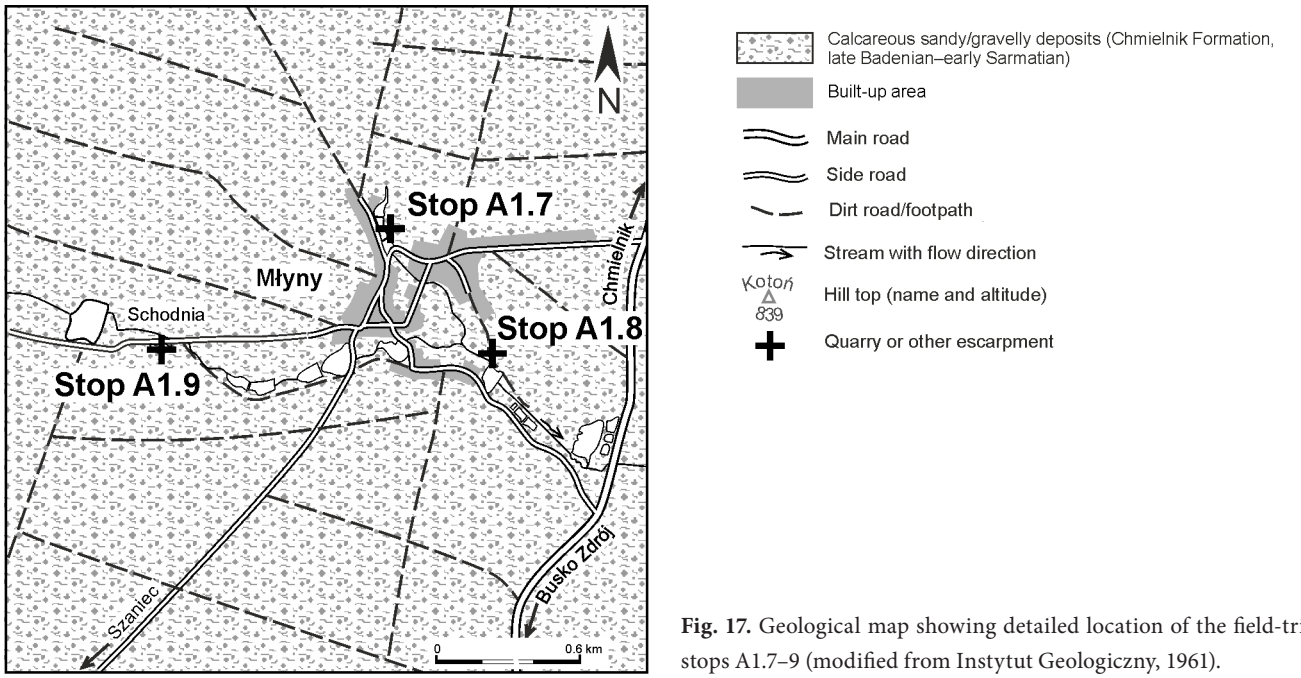

Fig. 17. Geological map showing detailed location of the field-trip stops A1.7–9 (modified from Instytut Geologiczny, 1961).

the sea and filled by a gravelly Gilbert-type bayhead delta (Fig. 19A) – all eventually drowned by a major marine transgression (see Fig. 5C–E). The lowstand shoal-water delta corresponding to the phase of valley incision is poorly exposed about 1.6 km to the south (Fig. 20; locality not included in this trip).

The incised valley-fill at stop A1.7 reaches 5 m in thickness and is estimated to be ca. 40 m wide. The south-

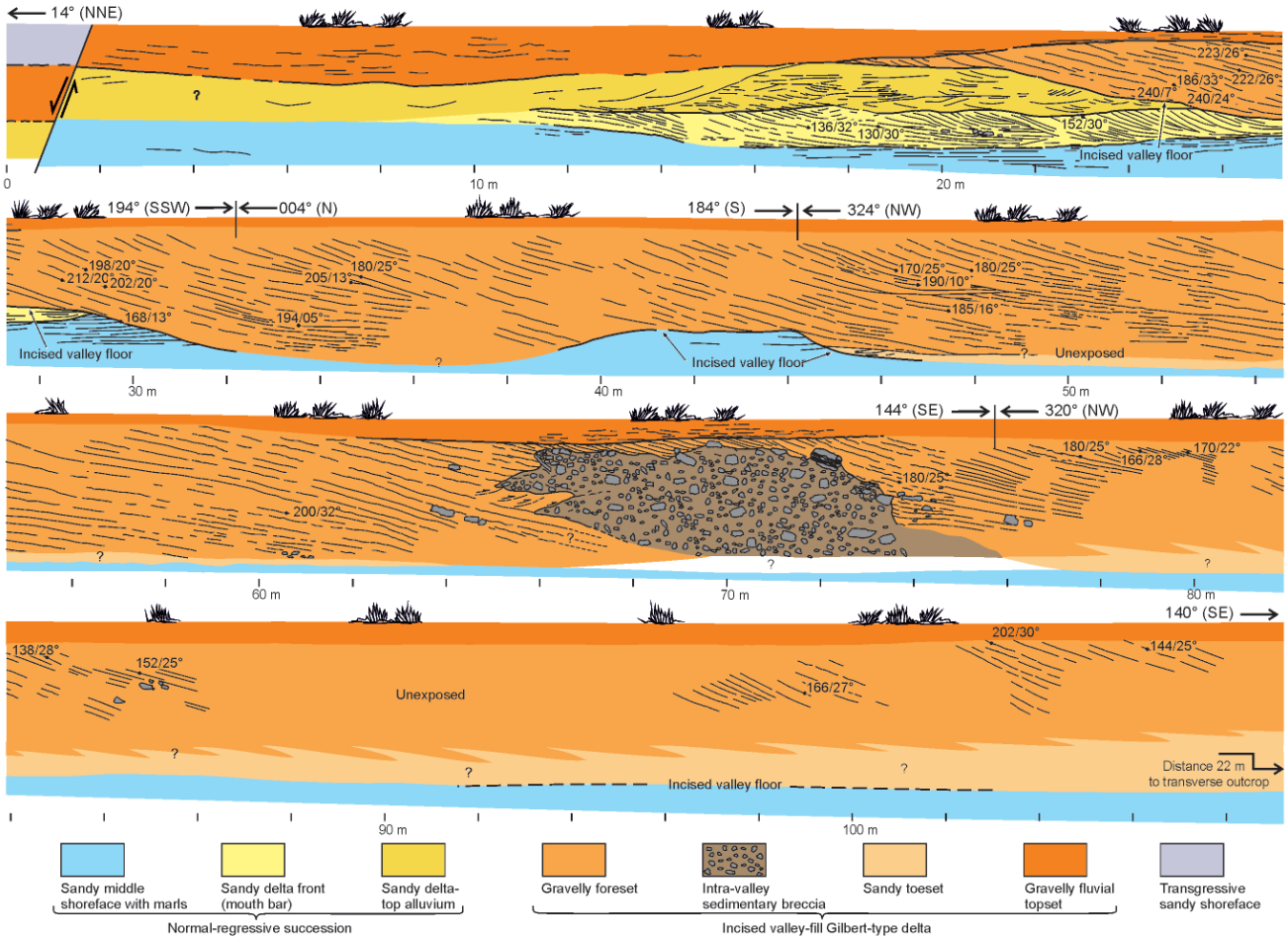

Fig. 18. A photomosaic overlay line-drawing of bedding architecture in the longitudinal outcrop section at stop A1.7 (Figs 1B, 17), approximately parallel to the incised palaeovalley. The numerical values on outcrop are the strata dip azimuth and angle. For facies interpretation, see legend. From Leszczyński and Nemec (2015).

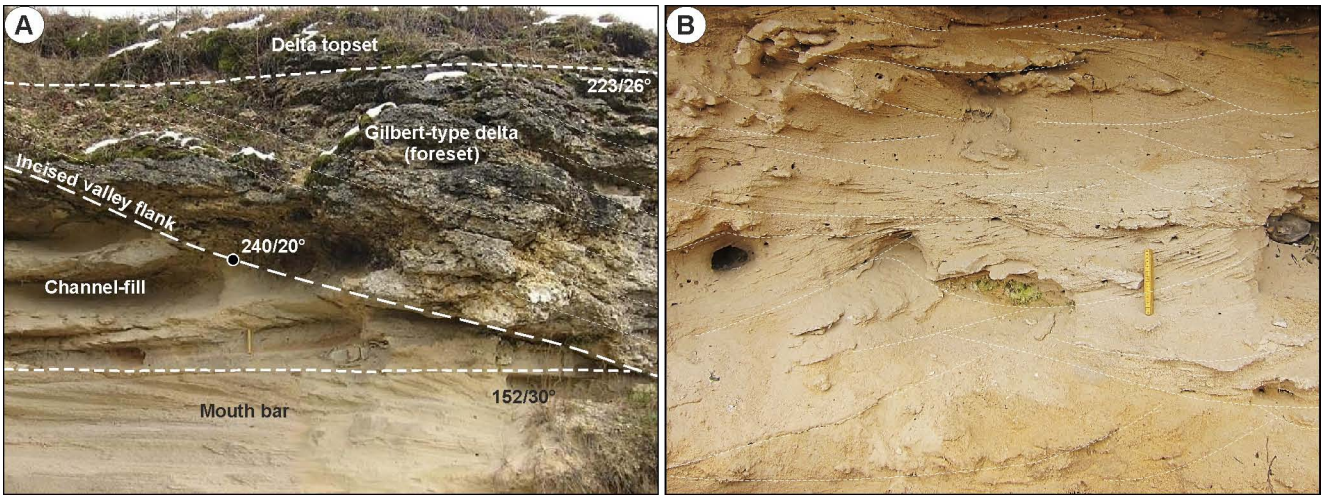

Fig. 19. (**A**) Deposits of a sandy shoal-water delta exposed beneath the incised palaeovalley floor at stop A1.7 (Figs 1B, 17 and 18, upper panel). Note also the nucleation point of the overlying valley-fill Gilbert-type delta. (**B**) Bedding architecture in the transverse outcrop section at stop A1.7 (Figs 1B, 17), approximately perpendicular to the incised palaeovalley, located 22 m to the south of the longitudinal section shown in Fig. 18. The delta foreset here is dipping towards the viewer. The photograph shows details of the delta-toe sandstones with spoon-shaped scour-and-fill strata sets cross-cutting one another; the yellow measuring stick (scale) is 12 cm.

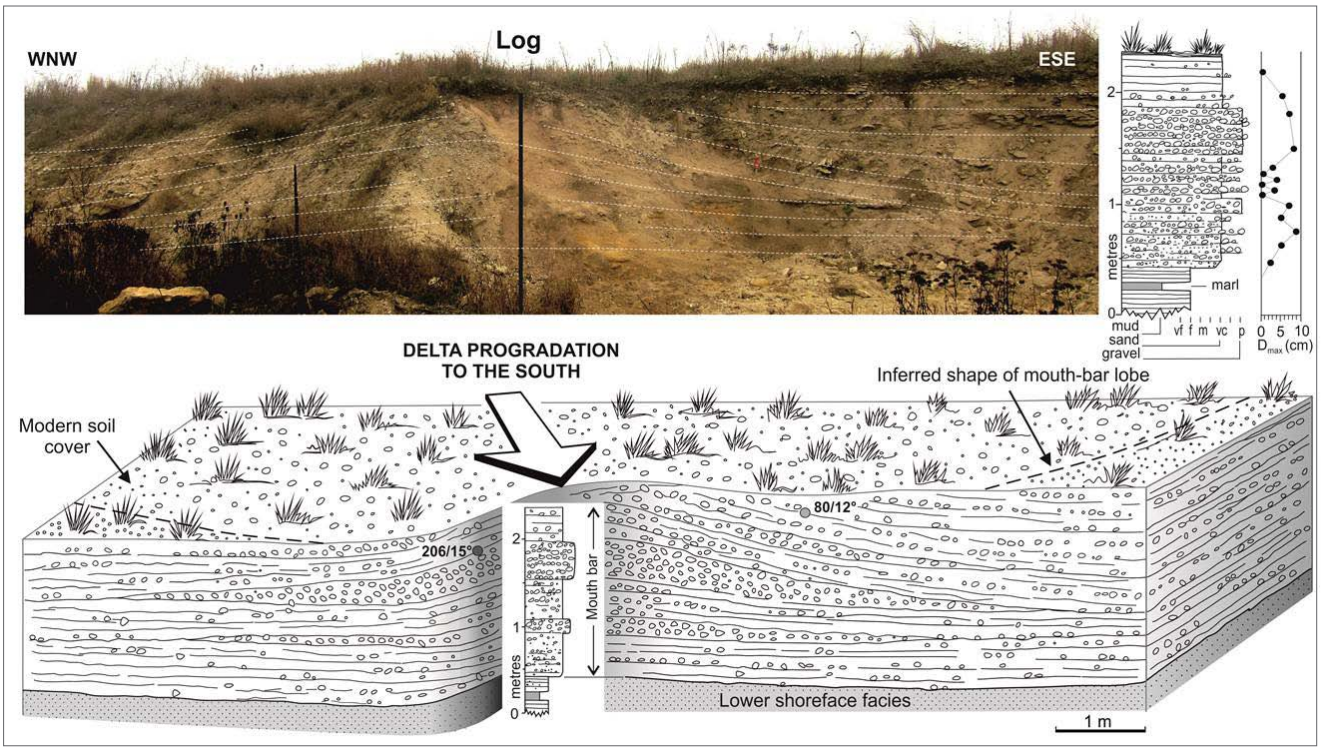

Fig. 20. Mouth bar of a gravelly shoal-water lowstand delta formed at the southern extension of the incised valley seen at stop A1.7. Outcrop at locality 12 in Fig. 5D, south of A1.7, not included in the excursion programme. From Leszczyński and Nemec (2015).

ward progradation of valley-filling delta was disturbed by a gravitational collapse of the valley's undercut western wall, recorded as a large mound of sedimentary breccia (Fig. 18, lower middle panel; see also Plate 3 and discussion in Leszczyński and Nemec, 2015). In a transverse outcrop section, the delta-toe pebbly sandstones show multiple scoop-shaped scour-and-fill features, 40–70 cm deep and a few metres wide, cross-cutting one another (Fig. 19B). Similar features, resembling trough cross-stratification and referred to as 'spoon-shaped depressions', were recognized at the toes of many modern and ancient Gilbert-type deltas (e.g., Breda *et al.*, 2007, 2009).

Stop A1.8 Escarpment along another fish pond in the south-eastern part of Młyny, less than 1km SE of previous stop

(50° 32′52″ N; 20° 43′50″ E; Fig. 17); access by footpath through private farm.

The small outcrops here – lateral to that at stop A1.7 – show a regressive shoreface to foreshore succession corresponding to the shoal-water delta and subsequent lowstand phase at the previous locality. The succession shows further the record of a brief marine transgression, coeval with the drowning of the incised valley at locality A1.7, followed by rapid shoreline progradation coeval with the advance of Gilbert-type bayhead delta at this adjacent locality (for outcrop details, see Leszczyński and Nemec, 2015, fig. 14).

Stop A1.9 An abandoned quarry in the hamlet of Schodnia, west of Młyny

(50°32′56″ N, 20°42′40″ E; Fig. 17); outcrop on the S side of local asphalt road

The quarry western wall, 4 m high (Fig. 21A), shows regressive foreshore deposits at the southern reaches of the mid-Serravalian regressive shoreline (see Fig. 5D) overlain by a gravelly transgressive lag and sandy transgressive shoreface deposits. The foreshore (strandplain) deposits form a foreset of steeply southwards-inclined granule to pebbly very coarse sand (Fig. 21B), underlain by coarse-sand upper-shoreface deposits (Fig. 21, log). The foreshore deposits are erosionally overlain by a transgressive lag of coarse-pebble gravel with small cobbles and numerous intraformational clasts (Fig. 21C). The overlying pebbly sandstones include an isolated set of planar cross-strata, ca. 70 cm thick, dipping towards the WSW (Fig. 21, log) and probably representing a longshore bar (see Allen, 1982). The overlying fining-upwards sandstones (Fig. 21, log) represent a transgressive shoreface succession (a relatively rare case, seldom reported from stratigraphic record, as most marine transgressions are erosive, rather than depositional).

Stop A1.10 Escarpment behind the roadside inn 'Leśna Chata' near Skorzów

(50°31′51″ N, 20°43′48″ E; Fig. 22)

The outcrop shows regressive shoreface deposits of a wave-worked, shoal-water spit platform at the distal eastern tip of a younger spit system formed farther to the south (Fig. 5D, E). The medium- to coarse-grained, parallel-stratified sandstones are inclined at 15–18° to the ESE and show at least one major surface of erosion and reactivation (Fig. 23A). Such an unusually high shoreface

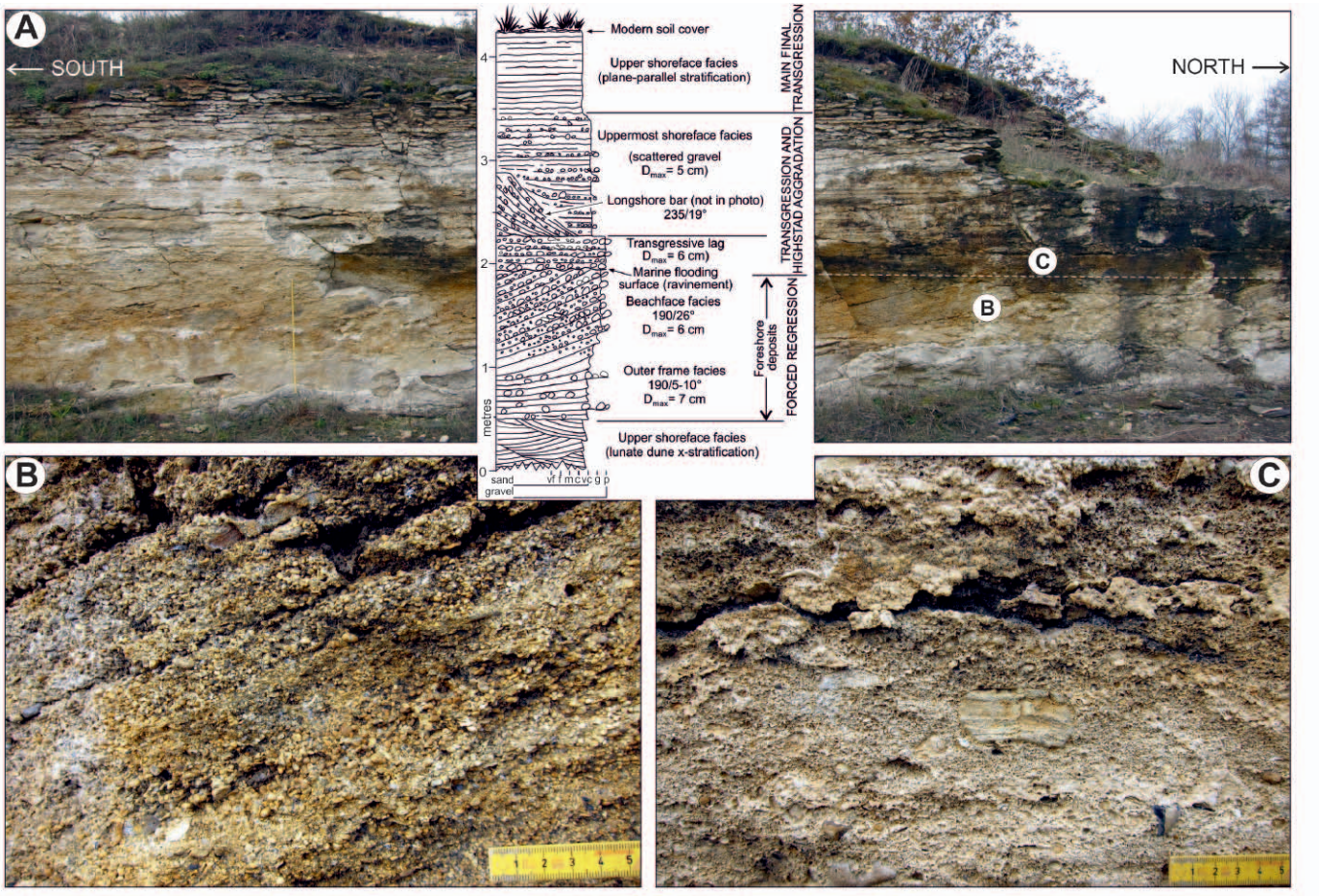

Fig. 21. (**A**) Outcrop photograph and a corresponding interpreted log of the deposits exposed at stop A1.9 (Figs 1B, 17). The yellow measuring stick is 1 m. The numerical values in the log are the strata dip azimuth and angle, and D_{max} is the maximum clast size. The close-up details show: (**B**) the cross-stratified well-sorted foreshore granule gravel and (**C**) the weakly planar-stratified transgressive gravel lag with scattered flat-lying marlstone clasts; the visible part of measuring stick is 5.5 cm.

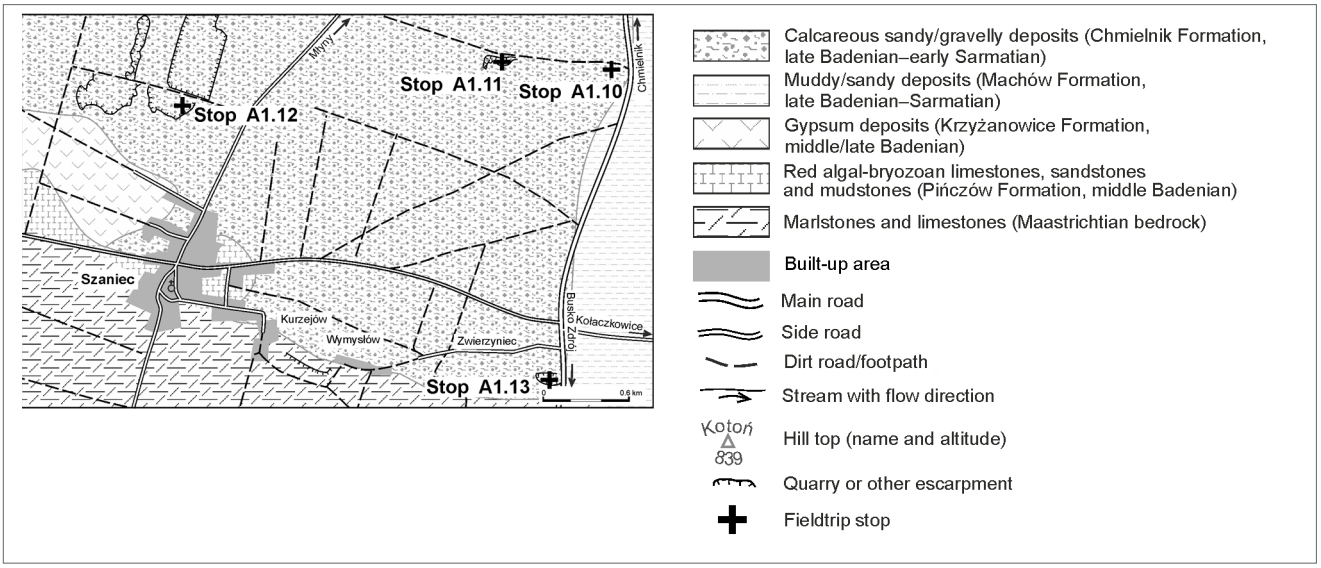

Fig. 22. Geological map showing detailed location of the field-trip stops A1.10–13 (modified from Instytut Geologiczny, 1961).

inclination is characteristic of spit platforms (see Plate 2B; Nielsen and Johannessen, 2008). The surface of erosion and reactivation is attributed to a rare violent storm event. The underlying fine-grained, parallel-stratified and wave-ripple cross-laminated sandstones show thin mudstone interlayers, indicating lower shoreface onto which the spit system advanced (see Fig. 23B).

Stop A1.11 Abandoned quarry 800 m to the west of stop A1.10

(50°31′52″ N, 20°43′12″ E; see Fig. 22); access by footpath from 'Leśna Chata' along a small valley.

The outcrop shows slightly more proximal deposits of the same late-stage spit system (Fig. 23B). Regressive upper-shoreface sandstones of the spit platform are

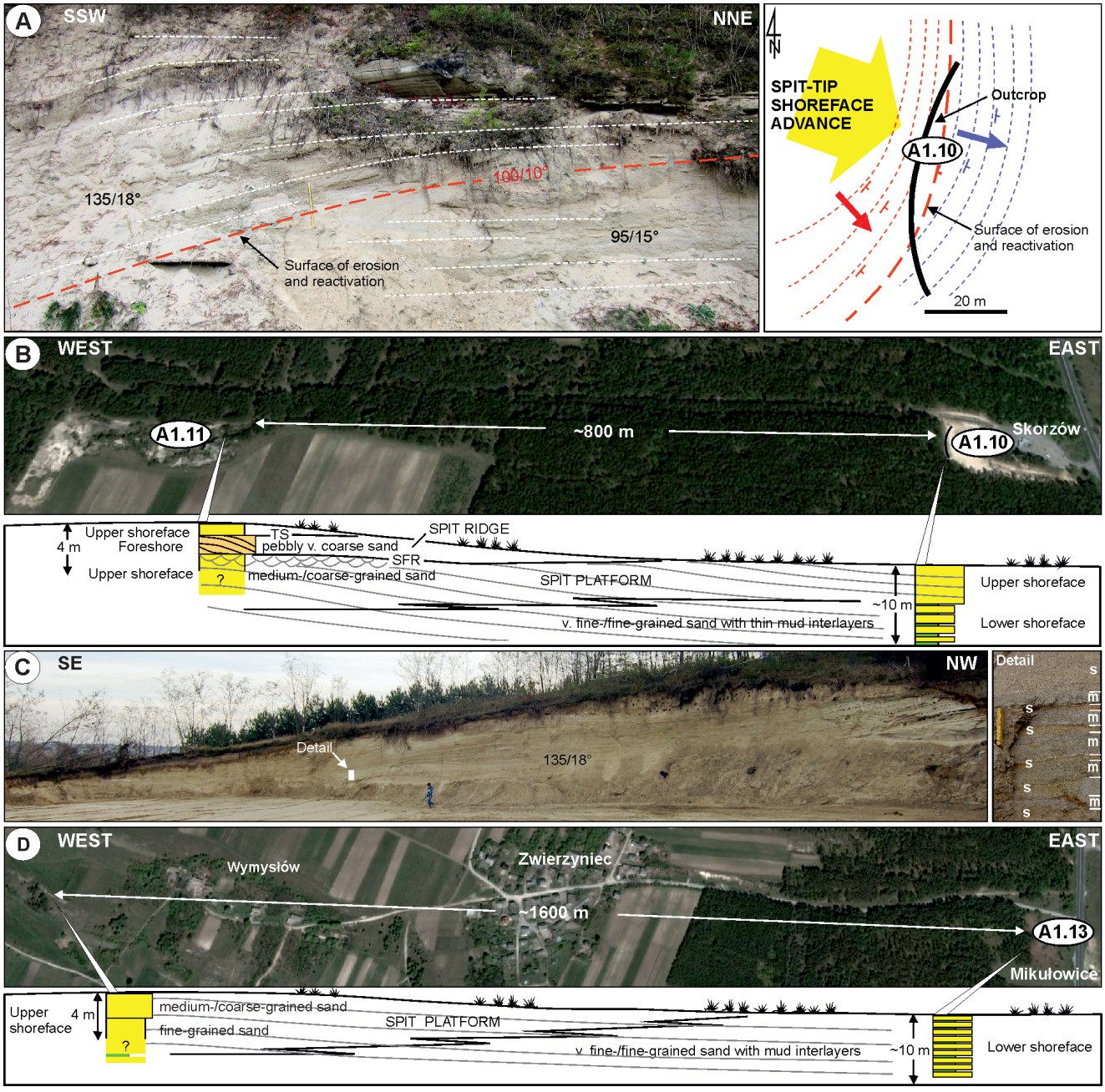

Fig. 23. (**A**) Wave-worked upper shoreface sandstones of the ESE-extended spit platform at stop A1.10 (Figs. 1B, 22); the relatively steep shoreface here was truncated by storm erosion and reactivated by spit re-advance (see the inset plan-view sketch of strata attitude). (**B**) Correlation of the spit-platform deposits at stop A1.10 with those at stop A1.11 (Figs 1B, 22), where the spit-ridge foreshore facies overlie spit-platform shoreface sandstones and are transgressively covered by similar shoreface facies. Letter symbols: SFR – surface of forced regression; TS – transgression surface. (**C**) Clinoform-bedded lower shoreface deposits at the southern flank of the same spit platform, exposed at stop A1.13 (Figs 1B, 22); the inset outcrop detail shows wave-worked fine-grained sandstones (s) intercalated with thin mudstone (m) and sporadic marlstone layers. (**D**) Correlation of the deposits at stop A1.13 with the upper-shoreface sandstones of spit platform exposed ca. 1.6 km to the west in the village of Wymysłów (Fig. 22). Land surface images from Google Earth. From Leszczyński and Nemec (2015).

overlain by spit-ridge pebbly foreshore sandstones (2 m thick) of the east-advancing spit bar. Foreshore strata are inclined at 15–20° to the ESE, with numerous flatter (5–10°) reactivation surfaces attributed to storm wave erosion. A gravel-paved ravinement surface and transgressive shoreface deposits at the top (Fig. 23B) are record of marine drowning – coeval with the ultimate transgression at stop A1.9.

Stop A1.12 Abandoned quarry on the hill Góra Kamnica north of Szaniec

(50°31′45″ N; 20°41′23″ E; Fig. 22); access by a short (400 m) dirt road to the W of the asphalt road Szaniec–Młyny

The deposits here represent an early development stage of the same southern spit system (stops A1.10 and A1.11), when it was initially dominated by tidal currents (Fig. 5C). The spit-ridge deposits are a succession of medium- to coarse-grained sandstones, ca. 3 m thick, with bidirectional (E–W) dune cross-stratification. They are underlain by poorly exposed spit-platform sandstones inclined eastwards at ca. 10° and showing plane-parallel stratification with subordinate wave-ripple cross-lamination and trough cross-stratification. The platform shoreface deposits, apparently uplifted by a local minor fault, are better exposed on the opposite side of the quarry.

Stop A1.13 Sand pit between the villages of Mikułowice and Zwierzyniec

(50°30′47″ N; 20°43′27″ E; Fig. 22), on the W side of main road 73.

The outcrop (Fig. 23C) shows regressive lower-shoreface deposits of distal spit platform (Fig. 23D) on the southern flank of the same spit system as seen at stops A1.10–12 (Fig. 22C, D). Characteristic is the unusual steep inclination (up to 18°) of the fine-grained, parallel-stratified and wave-ripple cross-laminated sandstones with thin mudstone interlayers. Microfauna is marine, but the deposits include horizons rich in terrestrial and freshwater gastropods. The malacofauna comprises aquatic and typical hygrophilous elements from coastal wetland habitats, some xerophilous species from dry open environments and gastropods from subtropical woodland (Stworzewicz *et al.*, 2013). The non-marine fauna was apparently derived from land by rain-wash and spread episodically by storms and tidal currents. The northern Paratethys in mid-Serravalian experienced the first spell of relatively warm and rainy climatic conditions heralding the Tortonian phases of 'washhouse' climate (Böhme *et al.*, 2008).

References

Agarwal, K., Singh, I., Sharma, M., Sharma, S. & Rajagopalan, G., 2002. Extensional tectonic activity in the cratonward parts (peripheral bulge) of the Ganga Plain foreland basin, India. *International Journal of Earth Science,* 91: 897–905.

Alexandrowicz, S.W., Garlicki, A. & Rutkowski, J., 1982. Podstawowe jednostki litostratygraficzne miocenu zapadliska przedkarpackiego. *Kwartalnik Geologiczny*, 26: 470–471. [In Polish.]

Allen, J. R. L., 1982. *Sedimentary Structures: Their Character and Physical Basis, Volume 2. Developments in Sedimentology*, 30B. Elsevier, Amsterdam, 643 pp.

Allen, P. A. & Allen, J. R., 2005. *Basin Analysis: Principles and Applications*. 2nd Edn, Blackwell Publishing, Oxford, 549 pp.

Beaumont, C., 1981. Foreland basins. *Geophysical Journal of the Royal Astronomical Society*, 65: 291–329.

Bluck, B. J., 1999. Clast assembling, bed-forms and structure in gravel beaches. *Transactions of the Royal Society of Edinburgh, Earth Sciences*, 89: 291–323.

Böhme, M., Ilg, A. & Winklhofer, M., 2008. Late Miocene "washhouse" climate in Europe. *Earth and Planetary Science Letters*, 275: 393–401.

Breda, A., Mellere, D. & Massari, F., 2007. Facies and processes in a Gilbert-delta-filled incised valley (Pliocene of Ventimiglia, NW Italy). *Sedimentary Geology*, 200: 31–55.

Breda, A., Mellere, D., Massari, F. & Asioli, A., 2009. Vertically stacked Gilbert-type deltas of Ventimiglia (NW Italy): the Pliocene record of an overfilled Messinian incised valley. *Sedimentary Geology*, 219: 58–76.

Catuneanu, O., Hancox, P. J. & Rubidge, B. S., 1998. Reciprocal flexural behaviour and contrasting stratigraphies: a new basin development model for the Karoo retro-

arc foreland system, South Africa. *Basin Research*, 10: 417–439.

Catuneanu, O. & Sweet, A. R., 1999. Maastrichtian–Paleocene foreland-basin stratigraphies, western Canada: a reciprocal sequence architecture. *Canadian Journal of Earth Sciences*, 36: 685–703.

Clifton, H. E., 1981. Progradational sequences in Miocene shoreline deposits, southeastern Caliente Range, California. *Journal of Sedimentary Petrology*, 51: 165–184.

Clifton, H. E. & Dingler, J. R., 1984. Wave-formed structures and paleoenvironmental reconstruction. *Marine Geology*, 60: 165–198.

Clifton, H. E., Hunter, R. E. & Phillips, R. L., 1971, Depositional structures and processes in the non-barred high energy nearshore. *Journal of Sedimentary Petrology*, 41: 651–670.

Currie, B. S., 1997. Sequence stratigraphy of nonmarine Jurassic–Cretaceous rocks, central Cordilleran foreland-basin system. *Geological Society of America Bulletin*, 109: 1206–1222.

Czapowski, G., 1984. Osady barierowe w górnym miocenie południowego obrzeżenia Gór Świętokrzyskich. *Przegląd Geologiczny,* 32: 185–194. [In Polish, with English summary.]

Czapowski, G., 2004. Otoczenie Gór Świętokrzyskich. In: Peryt, T. M. & Piwocki, M. (eds), *Budowa Geologiczna Polski, Tom I. Stratygrafia, Część 3a: Kenozoik*. Państwowy Instytut Geologiczny, Warszawa, pp. 239–245. [In Polish.]

Czapowski, G. & Studencka, B., 1990. Studium sedymentologiczno-paleontologiczne osadów barierowych dolnego sarmatu w rejonie Chmielnika (południowe obrzeżenie Gór Świętokrzyskich). *Przegląd Geologiczny*, 38: 117–126. [In Polish, with English summary.]

DeCelles, G. P. & Currie, B. S., 1996. Long-term sediment accumulation in the Middle Jurassic–early Eocene Cordilleran retroarc foreland-basin system. *Geology*, 24: 591–594.

De Leeuw, A., Bukowski, K., Krijgsman, K. & Kuiper K. F., 2010. Age of the Badenian salinity crisis; impact of Miocene climate variability on the circum-Mediterranean region. *Geology*, 38: 715–718.

Dudziak, J. & Łaptaś, A., 1991. Stratigraphic position of Miocene carbonate-siliciclastic deposits near Chmielnik (Świętokrzyskie Mountains area, central Poland) based on calcareous nannofossils. *Bulletin of the Polish Academy of Sciences, Earth Sciences*, 39: 55–66.

Dumas, S. & Arnott, R. W. C., 2006. Origin of hummocky and swaley cross-stratification – the controlling influence of unidirectional current strength and aggradation rate. *Geology*, 34: 1073–1076.

Dziadzio, P., 2000. Sekwencje depozycyjne w utworach badenu i sarmatu w SE części zapadliska przedkarpackiego. *Przegląd Geologiczny*, 48: 1124–1138. [In Polish, with English abstract.]

Dziadzio, P., Maksym, A. & Olszewska, B., 2006. Sedymentacja utworów miocenu we wschodniej części zapadliska przedkarpackiego. *Przegląd Geologiczny*, 54: 413–420. [In Polish, with English abstract.]

Ettensohn, F. R., 1994. Tectonic control on formation and cyclicity of major Appalachian unconformities and associated stratigraphic sequences. In: Dennison, J. M. & Ettensohn, F. R. (eds), *Tectonic and Eustatic Controls on Sedimentary Cycles. SEPM Concepts in Sedimentology and Paleontology*, 4: 217–242.

Flemings, P. B. & Jordan, T. E., 1989. A synthetic stratigraphic model of foreland basin development. *Journal of Geophysical Research*, 94 (B4): 3853–3866.

Flemings, P. B. & Jordan, T. E., 1990. Stratigraphic modeling of foreland basins: interpreting thrust deformation and lithosphere rheology. *Geology*, 18: 430–434.

Garecka, M. & Olszewska, B., 2011. Correlation of the Middle Miocene deposits in SE Poland and western Ukraine based on foraminifera and calcareous nannoplankton. *Annales Societatis Geologorum Poloniae*, 81: 309–330.

Górka, M., 2008. „Sarmat detrytyczny" wschodniego Ponidzia: litofacje i środowiska sedymentacji. In: Wojewoda, J. (ed.), *Baseny śródgórskie: kontekst regionalny środowisk i procesów sedymentacji*. Materiały konferencyjne POKOS'3 (Kudowa Zdrój). WIND, Wrocław, pp. 5–6. [In Polish.]

Hampson, G. J., 2000. Discontinuity surfaces, clinoforms, and facies architecture in a wave-dominated, shoreface–shelf parasequence. *Journal of Sedimentary Research*, 70: 325–340.

Helland-Hansen, W., 2009. Towards the standardization of sequence stratigraphy: Discussion. *Earth-Science Reviews*, 94: 95–97.

Hilgen, F. J., Lourens, L. J., Van Dam, J. A., Beu, A. G., Boyes, A. F., Cooper, R. A., Krijgsman, W., Ogg, J. G., Piller, W. E. & Wilson, D. S., 2012. The Neogene Period.

In: Gradstein, F. M., Ogg, J. G., Schmitz, M. D. & Ogg, G. M. (eds), *The Geologic Time Scale 2012*. Elsevier, Amsterdam, pp. 923–978.

Instytut Geologiczny, 1961. *Mapa geologiczna regionu świętokrzyskiego bez utworów czwartorzędowych 1:200 000*. Wydawnictwa Geologiczne, Warszawa.

Jasionowski, M., 1997. Zarys litostratygrafii osadów mioceńskich wschodniej części zapadliska przedkarpackiego. *Biuletyn Państwowego Instytutu Geologicznego*, 375: 43–60. [In Polish, with English abstract.]

Jasionowski, M., 2006. Facies and geochemistry of Lower Sarmatian reefs along the northern margins of the Paratethys in Roztocze (Poland) and Medobory (Ukraine) regions: paleoenvironmental implications. *Przegląd Geologiczny*, 54: 445–454. [In Polish, with English abstract.]

Jasionowski, M., Peryt T. & Czapowski, G., 2004. Miocen. In: Peryt, T. M. & Piwocki, M. (eds), *Budowa Geologiczna Polski, Tom I. Stratygrafia, Część 3a: Kenozoik*. Państwowy Instytut Geologiczny, Warszawa, pp. 213–224. [In Polish.]

Jordan, T. E. & Flemings, P. B., 1991. Large-scale stratigraphic architecture, eustatic variation, and unsteady tectonism: a theoretical evaluation. *Journal of Geophysical Research*, 96: 6681–6699.

Komar, P. D. & Miller, M., 1975. The initiation of oscillatory ripple marks and the development of plane-bed at high shear stresses under waves. *Journal of Sedimentary Petrology*, 45: 697–703.

Kováč, M., Nagymarosy, A., Oszczypko, N., Csontos, L., Ślączka, A., Marunteanu, M., Matenco, L. & Marton, E., 1998. Palinspastic reconstruction of the Carpathian–Pannonian region during the Miocene. In: Rakus, M. (ed.), *Geodynamic Development of the Western Carpathians.* Geological Survey of Slovak Republic, Dionyz Stur Publisher, Bratislava, pp. 189–217.

Kowalewski, K., 1958. Miocene stratigraphy of southern Poland with special attention paid to the southern margin of the Święty Krzyż Mountains. *Kwartalnik Geologiczny*, 2: 3–27. [In Polish, with English abstract.]

Kwiatkowski, S., 1972. Sedymentacja gipsów mioceńskich południowej Polski. *Prace Muzeum Ziemi*, 19: 3–94. [In Polish.]

Leszczyński, S. & Nemec, W., 2015. Dynamic stratigraphy of composite peripheral unconformity in a foredeep basin. *Sedimentology*, 62: 645–680.

Łaptaś, A., 1992. Giant-scale cross-bedded Miocene biocalcarenites at the northern margin of the Carpathian foredeep. *Annales Societatis Geologorum Poloniae*, 62: 149–167.

Łuczkowska, E., 1964. The micropaleontological stratigraphy of the Miocene in the region Tarnobrzeg-Chmielnik. *Prace Geologiczne Polskiej Akademii Nauk, Komitet Nauk Geologicznych*, 20: 1–72. [In Polish, with English summary.]

Massari, F. & Parea, G. C., 1988. Progradational gravel beach sequences in a moderate- to high-energy, microtidal marine environment. *Sedimentology*, 35: 881–913.

Meistrell, F. J., 1972. The spit-platform concept: laboratory observation of spit development. In: Schwartz, M. L. (ed.), *Spits and Bars*. Dowden, Hutchinson & Ross, Stroudsburg (PA), pp. 225–283.

Nielsen, L. H. & Johannessen, P. N., 2008. Are some isolated shelf sandstone ridges in the Cretaceous Western Interior Seaway transgressed, detached spit systems? In: Hampson, G. J., Steel, R. J., Burgess, P. M. & Dalrymple, R. W. (eds), *Recent Advances in Models of Siliciclastic Shallow-Marine Stratigraphy. SEPM Special Publications*, 90: 349–370.

Nielsen, L. H., Johannessen, P. N. & Surlyk, F., 1988. A Late Pleistocene coarse-grained spit-platform sequence in northern Jylland, Denmark. *Sedimentology*, 35: 915–937.

Olszewska, B., 1999. Biostratigraphy of Neogene in the Carpathian Foredeep in the light of new micropalaeontological data. *Prace Państwowego Instytutu Geologicznego,* 168: 9–28. [In Polish, with English abstract.]

Oszczypko, N., 1998. The Western Carpathian Foredeep – Development of a foreland basin in front of the accretionary wedge and its burial history (Poland). *Geologica Carpathica*, 40: 1–18.

Oszczypko, N., 2004. The structural position and tectonosedimentary evolution of the Polish Outer Carpathians. *Przegląd Geologiczny*, 52: 780–791.

Oszczypko, N., Krzywiec, P., Popadyuk, I. & Peryt, T., 2006. Carpathian Foredeep Basin (Poland and Ukraine): its sedimentary, structural and geodynamic evolution. In: Golonka, J. & Picha, F. J. (eds), *The Carpathians and Their Foreland: Geology and Hydrocarbon Resources. AAPG Memoirs,* 84: 293–350.

Oszczypko, N., Olszewska, B., Ślęzak, J. & Strzępka, J., 1992. Miocene marine and brackish deposits of the Nowy Sącz Basin (Polish Western Carpathians) – new lithostrati-

graphic and biostratigraphic standards. *Bulletin of the Polish Academy of Sciences, Earth Sciences*, 40: 83–96.

Peryt, D., 1987. Middle Miocene calcareous nannoplankton stratigraphy of the Roztocze region (SE Poland). *Bulletin of the Polish Academy of Sciences, Earth Sciences*, 35: 391–401.

Peryt, D., 1997. Calcareous nannoplankton stratigraphy of the Middle Miocene in the Gliwice area (Upper Silesia, Poland). *Bulletin of the Polish Academy of Sciences, Earth Sciences*, 45: 119–131.

Peryt, T. M., 2006. The beginning, development and termination of the Middle Miocene Badenian salinity crisis in Central Paratethys. *Sedimentary Geology*, 188-189: 379–396.

Piller, W. E., Harzhauser, M. & Mandic, O., 2007. Miocene Central Paratethys stratigraphy – current status and future directions. *Stratigraphy*, 4: 151–168.

Porębski, S. J., Pietsch, K., Hodiak, R. & Steel, R. J., 2003. Origin and sequential development of Upper Badenian–Sarmatian clinoforms in the Carpathian Foredeep Basin, SE Poland. *Geologica Carpathica*, 54: 119–136

Reuter, M., Piller, W. E. & Richoz, S., 2012. The dispersal of *Halimeda* in northern hemisphere mid-latitudes: palaeobiogeographical insights. *Perspectives in Plant Ecology, Evolution and Systematics*, 14: 303–309.

Rögl, F., 1998. Palaeogeographic considerations for Mediterranean and Paratethys seaways (Oligocene to Miocene). *Annalen des Naturhistorischen Museums in Wien,* 99A: 279–310.

Rögl, F., 1999. Mediterranean and Paratethys: facts and hypotheses of an Oligocene to Miocene paleogeography (short overview). *Geologica Carpathica,* 50: 339–349.

Rutkowski, J., 1976. Detrital Sarmatian deposits on the southern margin of the Holy Cross Mountains (southern Poland). *Prace Geologiczne*, Polska Akademia Nauk – Oddział w Krakowie, Komisja Nauk Geologicznych, 100: 71p. [In Polish, with English abstract.]

Rutkowski, J., 1981. The tectonics of miocene sediments of the western part of the Połaniec graben (Carpathian foredeep, southern Poland). *Annales Societatis Geologorum Poloniae*, 5l: 117–131. [In Polish, with English abstract.]

Sinclair, H. D., 1997. Tectonostratigraphic model for underfilled peripheral foreland basins: an Alpine perspective. *Geological Society of America Bulletin*, 109: 324–346.

Sinclair, H. D., Coakley, B. J., Allen, P. A. & Watts, A. B., 1991. Simulation of foreland basin stratigraphy using a diffusion model of mountain belt uplift and erosion: an example from the Central Alps, Switzerland. *Tectonics*, 10: 599–620.

Snedden, J. W. & Liu, C., 2010. A compilation of Phanerozoic sea-level change, coastal onlaps and recommended sequence designations. *AAPG Search and Discovery, Article* 40594, 3 pp.

Stachacz, M., 2007. Remarks on age of the Middle Miocene deposits in the Szydłów area (southern margin of the Holy Cross Mountains). *Przegląd Geologiczny,* 55: 168–174. [In Polish, with English abstract.]

Stworzewicz, E., Prisyazhnyuk, V. A. & Górka, M., 2013. Systematic and palaeoecological study of Miocene terrestrial gastropods from Zwierzyniec (southern Poland). *Annales Societatis Geologorum Poloniae*, 83: 179-200.

Wysocka, A., 1999. Depositional and tectonic controls on Early Badenian clastic sedimentation in the Sandomierz–Tarnobrzeg area (Baranów Beds, northern Carpathian Foredeep). *Geological Quarterly*, 43: 383–394.

Zastawniak, E., 1974. Die Blätterflora der sarmatischen Sedimente des südlichen Rendgebietes des Heiligenkreuzgebirge (Góry Świętokrzyskie, Mittel-Polen). In: Seneš, J. (ed.), *Chronostratigraphie und Neostratotypen. Miozän der Zentralen Paratethys, IV. M5*. Veda, Briatislava, pp. 663–665.

Zastawniak, E., 1980. Sarmatian leaf flora from the southern margin of the Holy Cross Mts. (south Poland). *Prace Muzeum Ziemi,* 33: 39–107.

The Organizing Committee would like to acknowledge the generous support of our Sponsors, Patrons, Partners and Exhibitors

Ministry of Science and Higher Education
Republic of Poland

Platinum Sponsor

ORLEN Upstream

Silver Partner

PGNiG
Polish Oil & Gas Company

Silver Sponsor

Springer

Patron

WIELICZKA SALT MINE

USB Flash-Drive Sponsor

WILEY

Writing-Pad & Writing-Pen Sponsor

SHALETECH ENERGY

Patron Sponsor

BETA
Radiocarbon Dating
Consistent Accuracy Delivered On-Time
Beta Analytic Ltd.

CoCaRDE

European Science Foundation

ZGM Bolesław

Muszynianka
naturalna woda mineralna

Lanyard Sponsor

ZEISS

Exhibitors

geokrak

SYL & ANT Instruments

INTROLIGATORNIA
Wiesław Nowotarski


2015
KRAKÓW